SQT

E83-10206

CR-170052

(E83-10206) AN OVERVIEW OF THE THEMATIC MAPPER GEOMETRIC CORRECTION SYSTEM (General Electric Co.) 89 p HC A05/MF A01 CSCL 08B

N83-22686

Unclas

G3/43 00206

AN OVERVIEW OF THE THEMATIC MAPPER GEOMETRIC CORRECTION SYSTEM

(DRAFT)

NAS5-25300

By: Eric P. Beyer
General Electric Company
Valley Forge Space Center
P.O. Box 8555
Phila., PA 19101

CONTENTS

I. INTRODUCTION

This paper summarizes the processing concepts which form the basis of the NASA Thematic Mapper (TM) Geometric Correction System.

TM geometric correction is a system process which includes both the Flight and Ground Segments. The principle Flight Segment subsystems are:

- Thematic Mapper
- Attitude Control
- Attitude Measurement
- On-Board Computer

The principle Ground Segment processes are:

- Payload Correction
- Control Point Processing
- Geometric Correction (Resampling)

1.1 Purpose and Fundamental Concept of Geometric Correction

The overall purpose of Geometric Correction is to place TM image samples onto an output coordinate system which is related to a map projection. This output product simplifies the data processing for subsequent applications. Conceptually, the geometric correction is accomplished in two phases: First, correction data is generated and then the raw TM image data is resampled using the correction data.

Figure 1-1 illustrates correction data generation. The spacecraft position, TM frame attitude, position of the TM scanning mirrors and detector sampling are known as a function of time, through a combination of Flight Segment measurements, Ground Segment modeling and control point information. This information, along with an earth geoid model, is used to determine the geoid location for each TM image sample (geoid look point). Then, using map projections, correction data can be generated which defines the location of each TM sample on the output coordinate system.

As with previous Landsats, products will be provided on an output grid system known as a World Reference System (WRS). The WRS is defined by a nominal orbit path. Each of the nominal 233 orbit paths of the sun synchronous Landsat-D orbit is divided into 248 WRS scenes. Including overlap with adjacent scenes in the same orbit, a scene is approximately 170 km along-track by 185 km across-track. A WRS scene is identified by a scene center latitude and longitude and a map rotation angle for each map projection. Output products can be provided in either of two map projections:

1. Space Oblique Mercator (SOM)
2. Universal Transverse Mercator when scene center is between 65 degrees South latitude and 65 degrees North latitude or Polar Stereographic when scene center is below 65 degrees South latitude and above 65 degrees North latitude.

The output coordinate system for all satellite passes over the WRS scene is the map projection coordinate system rotated about the WRS scene center location by the map rotation angle.

Figure 1-2 illustrates the resampling concept. The correction data is used to locate TM detector samples on the output coordinate system, and TM detector samples are then interpolated to the desired output grid locations.

FIGURE 1-1
CORRECTION DATA GENERATION CONCEPT

FIGURE 1-2

RESAMPLING CONCEPT

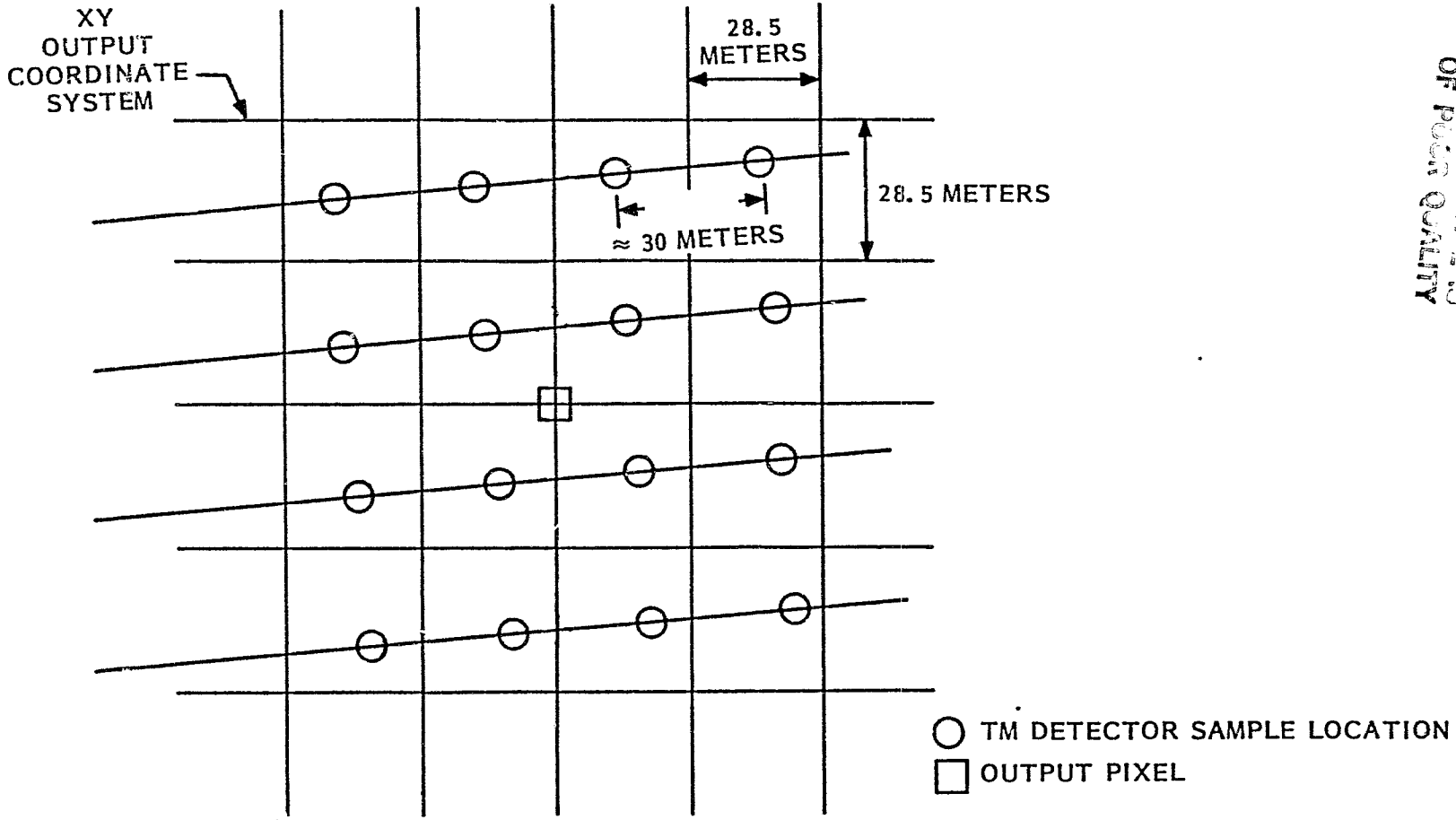

1.2 Geometric Accuracy

An overview of the Landsat-D geometric accuracy specifications are shown in Figure 1-3. Effectively, a reference interval (set of consecutively imaged scenes) is geodetically rectified to a set of maps. Registration control points are then extracted from the reference interval and stored in a control point library. Subsequently imaged intervals are registered to the reference interval using the control point library. There are three geometric accuracy requirements: Band-to-band registration, temporal registration and geodetic rectification.

Band-to-Band registration is the ability to overlay spectral bands within a single scene. It is considered the most important accuracy requirement. The Thematic Mapper band-to-band requirements are 0.2 pixel (90% of the time) between spectral bands on the same focal plane and 0.3 pixel (90% of the time) between spectral bands on primary and cold focal planes. A TM pixel is 42.5 microradians. Bands 1 to 4 are on the primary focal plane and Bands 5 to 7 are on the cold focal plane. With ground processing, these band-to-band accuracy requirements are expected to be easily satisfied.

Temporal registration is the ability to overlay a band of the registrant scene with the corresponding band of the reference scene. The accuracy requirement is 0.3 pixel (90% of the time). The temporal registration requirement is the most challenging system accuracy requirement. The following simplified calculation illustrates this point:

$$0.3 \text{ pixel temporal (90\%)} \times \frac{42.5 \text{ } \mu\text{rad}}{\text{pixel}} \times \frac{(1\sigma)}{1.645(90\%)} \times \frac{\text{Single scene}}{\sqrt{2} \text{ temporal}}$$

$$= 5.48 \text{ } \mu\text{rad } (1\sigma) \text{ single scene}$$

$$= 1.13 \text{ arc-sec } (1\sigma) \text{ single scene}$$

$$= 3.87 \text{ meter (at 705.3km) } (1\sigma) \text{ single scene}$$

FIGURE 1-3

GEOMETRIC ACCURACY SPECIFICATIONS

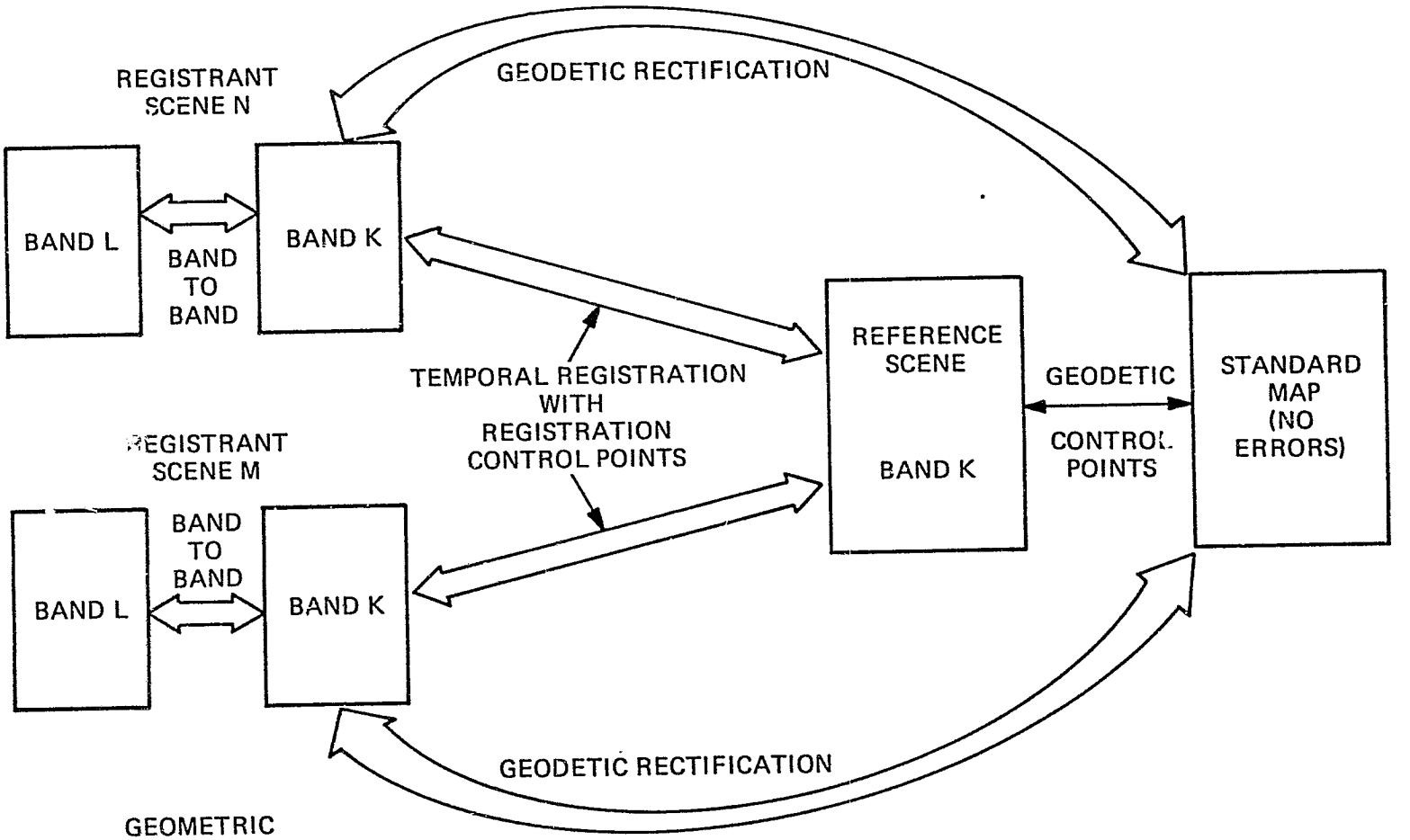

GEOMETRIC CORRECTION REQUIREMENTS 90% OF THE TIME

GEODETIC	0.5 PIXEL
TEMPORAL	0.3 PIXEL (REGISTRANT TO REFERENCE)
BAND-TO-BAND	0.3 PIXEL (BETWEEN PRIMARY AND COLD FOCAL PLANES)
	0.2 PIXEL (WITHIN EACH FOCAL PLANE)

That is, the 0.3 pixel 90% of the time accuracy between two scenes allows no more than 3.87 meters (1σ) total system error for one scene. This simplified calculation assumes that the error is Gaussian (the factor of 1/1.645 converts 90% to 1σ) and that the errors in the two scenes are uncorrelated (the factor of $1/\sqrt{2}$). The temporal registration accuracy requires an adequate number of ground control points. This may be as large as 18 control points when a single scene is processed, but can be reduced to 3 to 4 control points per scene when consecutive scenes from one orbit (an interval) are processed. The temporal registration accuracy will be discussed further in Section 4.0.

Geodetic rectification is the ability to overlay a band of the registrant scene with the original maps. The accuracy requirement is 0.5 pixel (90% of the time). This accuracy is to be met when the maps have no geometric errors, over regions without topological variations and given sufficient numbers of geodetic control points. To the extent that these conditions are not satisfied in actual operation, the geodetic accuracy of output products will degrade.

1.3 System Overview

An overview of NASA's Landsat-D TM Geometric Correction System is shown in Figure 1-4. The Flight Segment includes the TM instrument, attitude measurement devices, attitude control and ephemeris processing. The Flight Segment inertial attitude estimates are made using an extended Kalman Filter process, which corrects integrated gyro measurements using star tracker information. Attitude is controlled using reaction wheels. Ephemeris, used for attitude control and ground processing, is uplinked from the ground or determined using the on-board Global Positioning System. Attitude control and ephemeris processing are implemented in the on-board computer.

FIGURE 1-4

LANDSAT D TM GEOMETRIC CORRECTION SYSTEM OVERVIEW

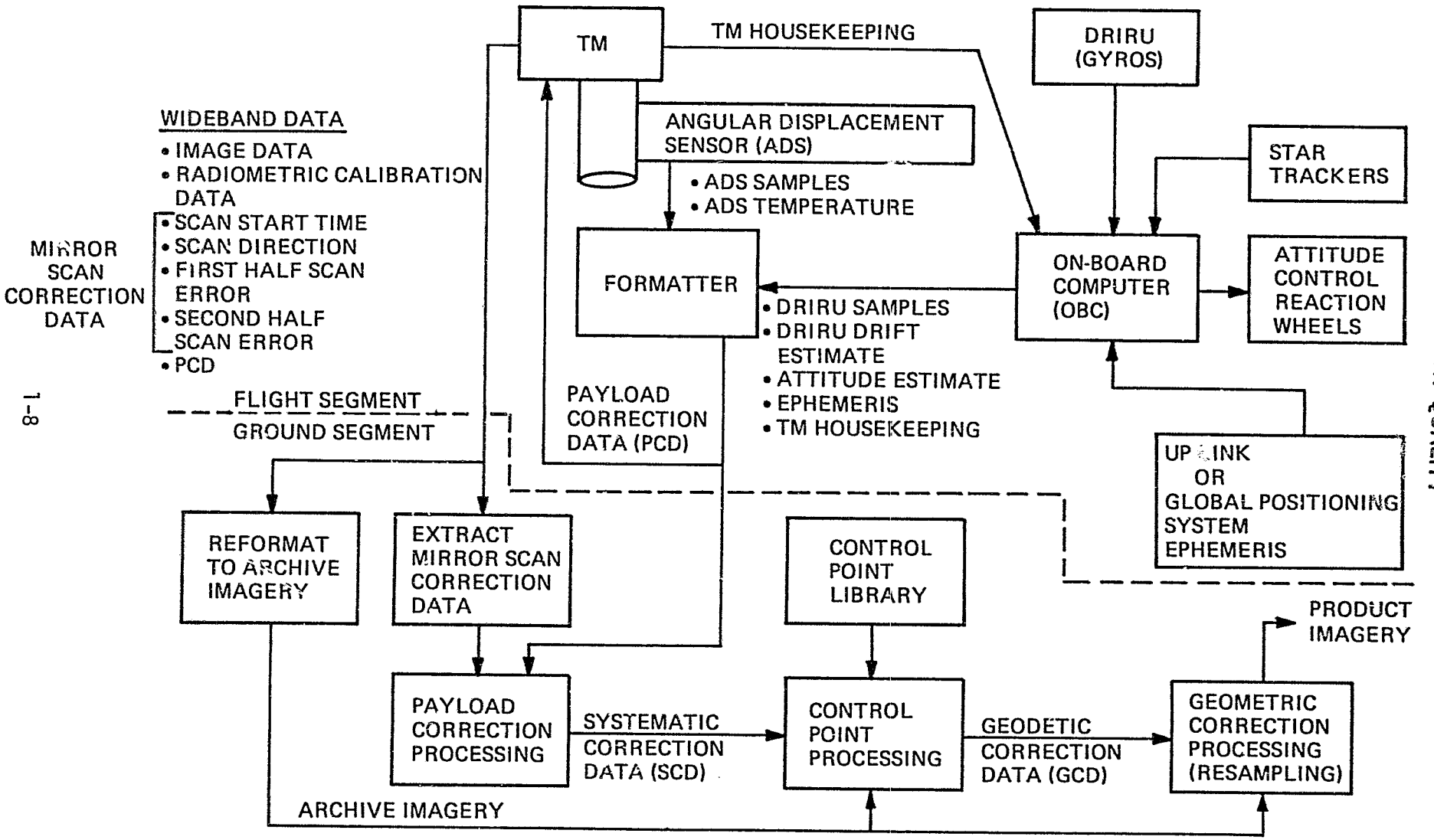

The spacecraft attitude is downlinked for ground processing but at a rate (4.096 seconds) that cannot follow all TM attitude deviations. Low frequency (0 to 2 Hz) attitude deviations are measured by gyro samples supplied every 0.064 seconds per axis. Higher frequency (2 to 125 Hz) attitude deviations are measured using Angular Displacement Sensors (ADS) which are sampled every 0.002 seconds per axis. The Angular Displacement Sensor is mounted directly on the Thematic Mapper.

A spacecraft formatter combines the necessary On-Board Computer information and the ADS samples into a 32 kilobit per second telemetry stream called Payload Correction Data (PCD). PCD contains all Flight Segment information needed to perform TM data processing. It is both downlinked on a telemetry channel and included with the TM wideband data. Also imbedded into TM wideband data is Mirror Scan Correction Data (MSCD) from which the scan mirror position as a function of time is determined. This data includes scan start time, scan direction, first half scan time error, and second half scan time error.

The NASA TM ground processing extracts the Mirror Scan Correction Data (MSCD) from the TM wideband data. The PCD is received using the telemetry path. Payload Correction Processing then combines the MSCD and PCD to generate Systematic Correction Data (SCD). The Systematic Correction Data is a complete set of correction data except that large bias and slow drift errors exist due to time, ephemeris, gyro measurement, attitude control and TM alignment uncertainty. These bias and drift errors are removed by Control Point Processing. Control Point Processing uses the mislocation between features in reference interval and the same features in the registrant interval to estimate these SCD errors. The SCD is then modified to remove the error effects and the result is called Geodetic Correction Data.

The payload correction and control point processing are performed over an interval or number of consecutively imaged scenes in an orbit path. This results in improved accuracy and fewer control points than processes that operate on individual scenes.

The final steps in geometric correction system involve resampling the TM image samples to place them onto the output coordinate system. The TM wideband data is first reformatted into Archive imagery in which reverse scan data has been reordered to correspond to the forward scan data, and integer detector and band offsets have been removed. The Archive imagery is then resampled during Geometric Correction Processing. The resampling is performed using the Geodetic Correction Data and it results in product imagery.

A more detailed description of the Flight Segment contributions to geometric correction is given in Section 2.0, the Ground Segment Processing is described in Section 3.0 and a system level temporal registration error budget is summarized in Section 4.0.

II. FLIGHT SEGMENT

The Landsat-D Flight Segment is shown in Figure 2-1. It is configured in two modules: Multimission Modular Spacecraft (MMS) and Instrument Module (IM). The MMS provides standard spacecraft subsystems such as Attitude Control (ACS), Propulsion Module for orbit adjust, a Collection and Data Handling (C&DH) Module which includes an On-Board Computer (OBC), and a Power Module. The Instrument Module includes the mission unique subsystems such as Thematic Mapper, Multispectral Scanner (MSS), Wideband Communications, High Gain Antenna and RF Compartment, Global Positioning (GPS) and Solar Array.

The Flight Segment contributions to geometric correction will be described in terms of TM position (ephemeris), TM attitude, TM scanning operation and associated Flight Segment correction information which is used in the Ground Segment Processing.

2.1 Position

TM inertial position is a factor in determining the TM sample location on the output coordinate system. Before describing how this knowledge is obtained (Section 2.1.2), the basic orbital parameters will be described.

Landsat-D Orbit

As shown in Figure 2-2, the Landsat-D orbit is sun synchronous, nominally crossing the equator at 9:45 a.m. local time. The orbit inclination is nominally 98.21 degrees with periodic orbit adjust maintaining this inclination to $\pm$.045 degrees. The nominal equatorial altitude is 705.3 kilometers and due to a combination of periodic orbital eccentricity and earth oblateness the altitude will vary from 696 to 741 kilometers. The ground track repeats on a 16-day cycle and the

FIGURE 2-1

LANDSAT D FLIGHT SEGMENT

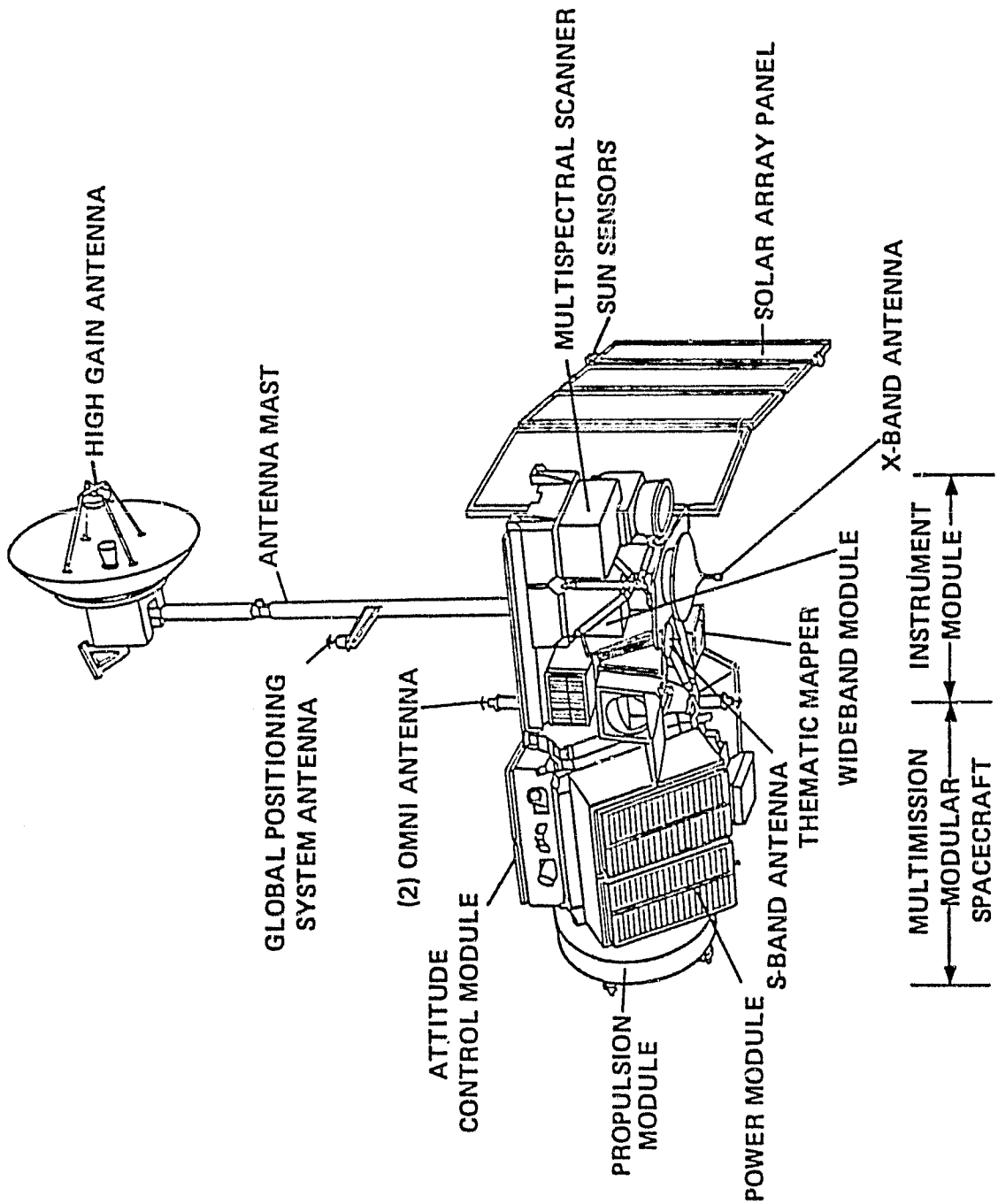

FIGURE 2-2

LANDSAT-D ORBIT

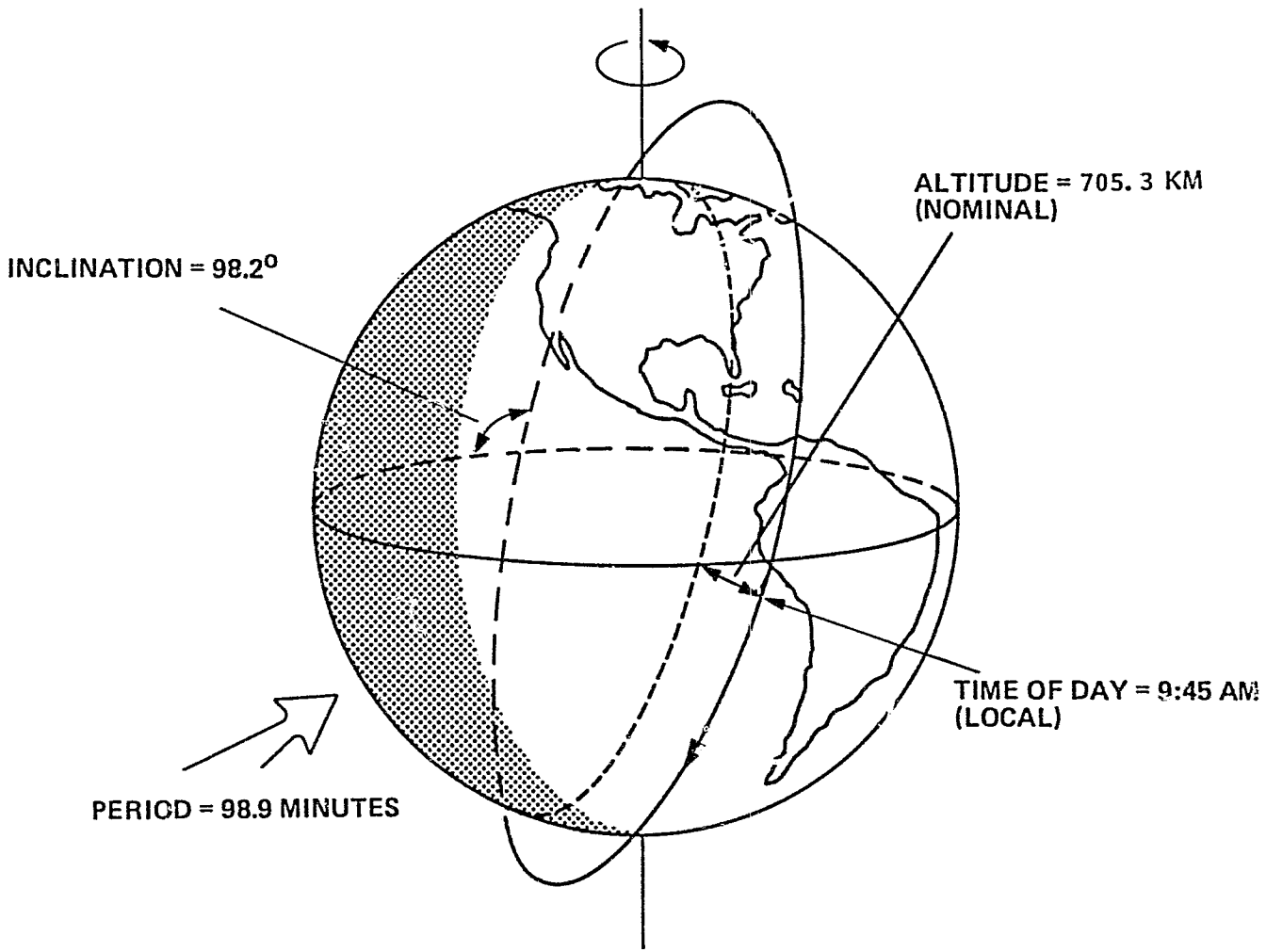

equatorial crossing is maintained to within ± 4 kilometers by periodic orbit adjust. The 16-day cycle generates 233 ground paths with a seven day skip-cycle between adjacent paths.

The orbit inclination drifts, orbit altitude variation and ground track variation have significant geometric impacts. Orbit inclination drift is a factor affecting image rotation requirements. Altitude variation effects ground sample distance, inter-scan gap and scan line skew (see Section 2.3). Ground track and altitude variations interact with earth topology to create temporal registration errors.

Ephemeris

Ephemeris is data which describes the position and velocity of the TM as a function of time. Landsat-D ephemeris data is obtained directly from downlinked Payload Correction Data (PCD) telemetry. A more detailed description of Payload Correction Data is given in Section 2.4.

A system level ephemeris data flow is given in Figure 2-3. There are two possible sources of ephemeris data: NASA Goddard Orbit Support Computing Division (OSCD) and the Global Positioning System (GPS). OSCD generates predicted Earth Centered Inertial (ECI) ephemeris, then converts it to a highly compressed Fourier power series and residuals representation. The compressed data is uplinked to the Flight Segment where the on-board computer reconstructs the ECI ephemeris.

A GPS receiver/processor assembly (R/PA) is an experimental subsystem which is part of the Flight Segment. The receiver/processor assembly uses ranging information from GPS satellites to estimate Landsat-D ephemeris. The GPS ephemeris is computed in Earth Centered Earth Fixed coordinates, then sampled, converted to ECI and extrapolated by the On-Board Computer.

FIGURE 2-3

SYSTEM EPHEMERIS DATA FLOW FOR TM GEOMETRIC CORRECTION

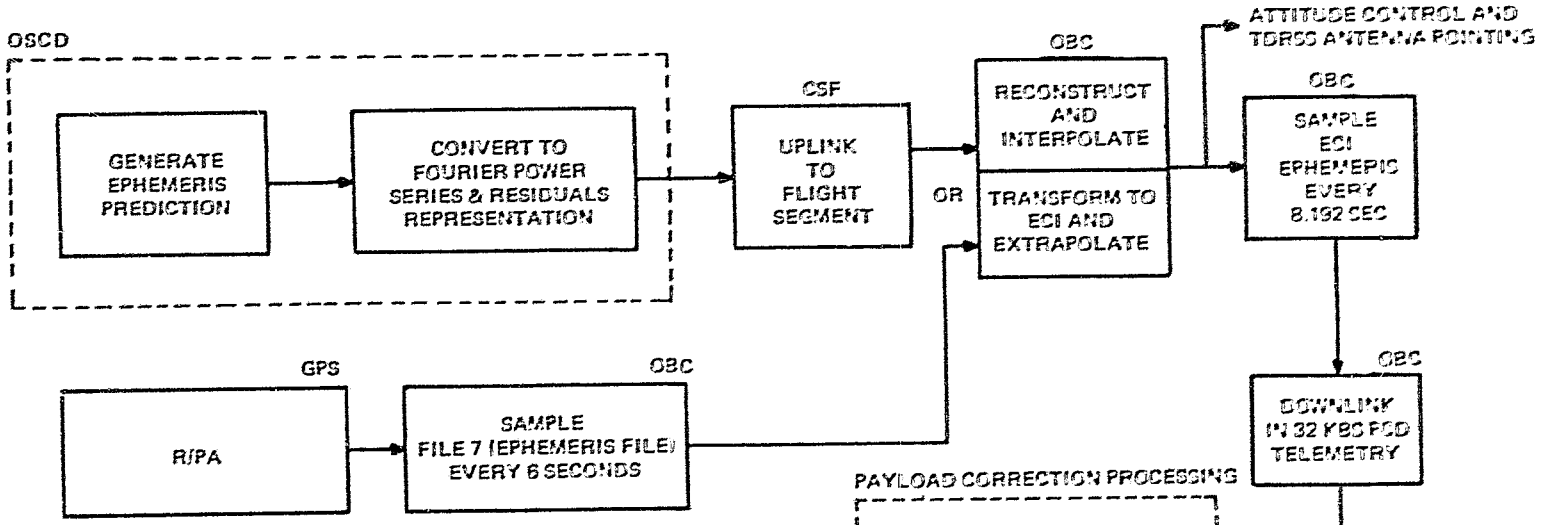

LEGEND

OSCD: ORBIT SUPPORT COMPUTING DIVISION

CSF: CONTROL AND SIMULATION FACILITY

OBC: ON-BOARD COMPUTER

MMF: MISSION MANAGEMENT FACILITY

EDP: EPHEMERIS DATA PROCESSING

ECI: EARTH CENTERED INERTIAL

GPS: GLOBAL POSITIONING SYSTEM

R/PA: RECEIVER PROCESSOR ASSEMBLY

J2: SECOND ZONAL HARMONIC

PCO: PAYLOAD CORRECTION DATA

TDRSS: TRACKING DATA RELAY SATELITE SYSTEM

Independent of the ephemeris source, the resulting ECI ephemeris is used for attitude control and pointing the TDRSS Antenna. The ephemeris is sampled every 8.192 seconds and formatted for downlink by the On-Board Computer. Once on the ground, the received ephemeris data is fitted with a J2 orbit model. This is done to remove GPS data discontinuities or processing errors caused by the compression and decompression of OSCD ephemeris. The ground ephemeris processing is discussed in Section 3.1 (Payload Correction Processing).

The downlinked OSCD ephemeris may be a two-day old prediction. After ground processing, the error standard deviation of such data is given below:

	Position (Meters)	Velocity (Meters/Second)
Along Track	500	.163
Cross-Track	100	.655
Radial	33	.650

The error standard deviation of GPS ephemeris is difficult to predict because it depends upon the number of operational GPS satellites and the length of time since the last GPS observation. GPS accuracy is expected to be considerably better than OSCD two-day predicts.

A +20 millisecond uncertainty in spacecraft time will result in an addition ±140 meter along-track positional uncertainty.

The geometric effect of ephemeris and time errors are estimated and corrected during control point processing. This processing is described in Section 3.2.

2.2 ATTITUDE

The TM attitude (orientation in an inertial frame of reference) is another factor used in determining the TM sample location on the output coordinate system. There are three dominant components which effect TM attitude: the Attitude Control Subsystem (ACS), higher frequency attitude deviations, and TM alignment with the Attitude Control Subsystem.

For discussion purposes, define the instrument coordinate system as shown below:

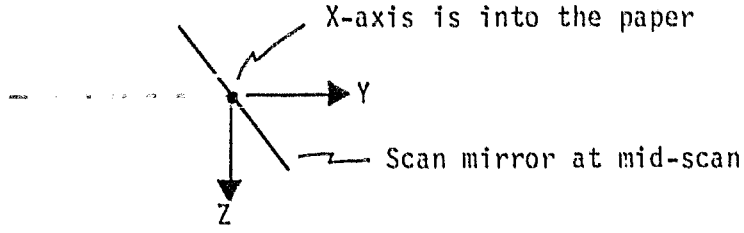

The X-axis is along the scan mirror pivot axis, the Z-axis is the telescope optical axis reflected through scan mirror at midscan, and the Y-axis completes the right hand coordinate system. Rotation about the X, Y and Z axes are called roll, pitch and yaw, respectively.

Such coordinate systems are defined for the TM and Multispectral Scanner (MSS) instruments. The instruments are mounted onto the Flight Segment such that the difference between the TM and MSS axes is less than 0.15 degrees in roll, 0.5 degrees in pitch, and 0.5 degrees in yaw. The alignments between the ACS axes and the TM axes and between the TM axes and MSS axes are then measured. Based on the available ECI ephemeris, the ACS controls the mean axes between the TM and MSS such that the mean Z-axis points to the earth center and the mean X-axis points along the instantaneous ephemeris velocity vector.

The ACS is a low frequency control system with bandwidths less than 0.01 Hz. Any higher frequency attitude deviations, which arise from the TDRSS antenna drive, the solar array drive, and TM or MSS mirror impacts, are not compensated by the ACS. Such disturbances must be measured and corrected in ground processing.

The ACS, alignments and high frequency attitude deviations are now described in more detail.

ATTITUDE CONTROL SYSTEM (ACS)

Figure 2-4 shows a simplified functional block diagram of the Landsat-D Attitude Control System. The DRIRU (gyros) and Fixed Head Star Trackers constitute the attitude measurement devices. The reaction wheels are used to effect attitude control. In ACS operation the DRIRU measures change in inertial attitude about each of its three axes every 0.064 seconds. Gyro Data Processing removes gyro drift and low pass filters the samples to a 0.5 Hz bandwidth. The Euler Parameter Integration propagates the ACS Attitude using the processed DRIRU increments every 0.512 seconds. The Update Filter implements an extended Kalman filter process which uses the attitude error between the propagated ACS attitude estimate and star tracker measurements to compute gyro drift and an attitude correction. Star tracker measurements are made at most every minute, but under worst case conditions tens of minutes may elapse between star measurements. Based on ECI ephemeris (see Section 2.1) and the alignment between the ACS axes and mean instrument axes, the desired ACS attitude is computed. The desired attitude has the mean TM & MSS instrument Z-axis pointed to the earth center and the mean instrument X-axis along the instantaneous velocity vector. An attitude error is computed and the reaction wheels are appropriately commanded every 0.512 seconds.

FIGURE 2-4

ATTITUDE CONTROL SUBSYSTEM (ACS)

NORMAL OPERATING MODE FUNCTIONAL BLOCK DIAGRAM

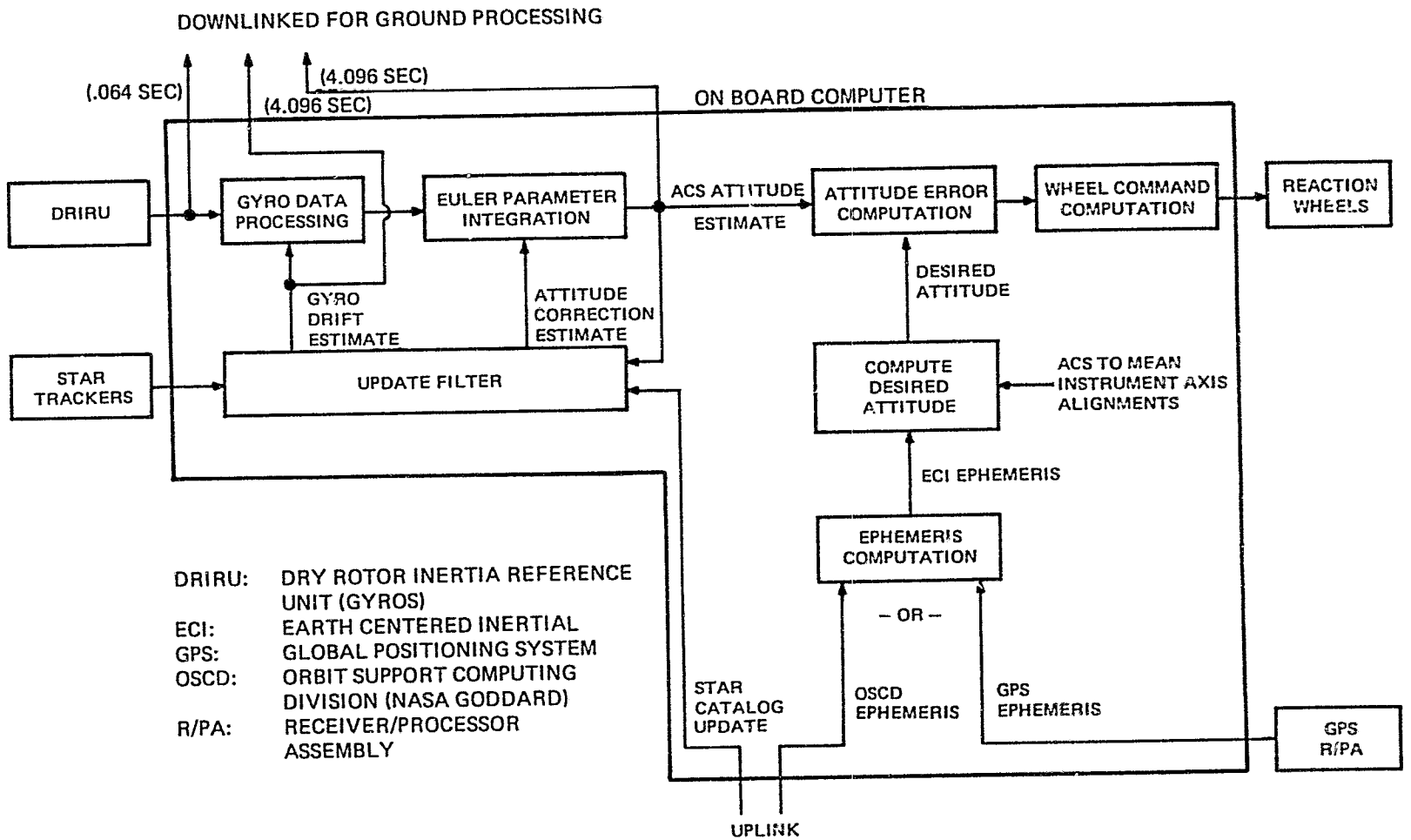

The ACS is a closed loop system because the attitude changes effected by the reaction wheels are sensed by the DRIRU. The ACS control bandwidth is 0.01 Hz about the pitch axis and 0.005 Hz about the roll and yaw axes. Exclusive of ephemeris error and disturbances caused by the TM and MSS, the ACS is required to control its pointed axes to within 0.01 degrees (1σ) with an attitude rate error of less than 10^{-6} degree/second (measured over a 100 minute interval). The dominant source of ACS error arises from Star Tracker measurement error.

As Figure 2-4 indicates, the DRIRU data (every 0.064 seconds), gyro drift estimate (every 4.096 seconds) and ACS attitude estimate (every 4.096 seconds) are down-linked for ground processing. Significant low frequency error exists in this data and their error effects must be removed during control point processing. These errors result from Star Tracker measurement errors, gyro drift estimation errors and propagated DRIRU Measurement Errors, and could be as large as 0.01 degrees (1σ) about the roll, pitch and yaw axes. Figure 2-5 shows typical error dynamics of DRIRU Measurements.

Alignment

The alignment between the ACS and the TM axes is a factor in determining the TM sample locations on the output coordinate system. ACS to TM alignment uncertainty results from error in the alignment measurement process in which eight separate alignment measurements are required. These measured alignments change as a result of launch structural stress, difference in thermal conditions between alignment measurements and orbital conditions, and spacecraft reassembly at the launch site. The ACS to TM alignment uncertainty will be 125 arc-sec (1σ) in roll and 250 arc-sec (1σ) in pitch and yaw. These alignment uncertainties will be substantially reduced by ground measurements using control points.

FIGURE 2-5

LOW FREQUENCY ATTITUDE ERROR DYNAMICS

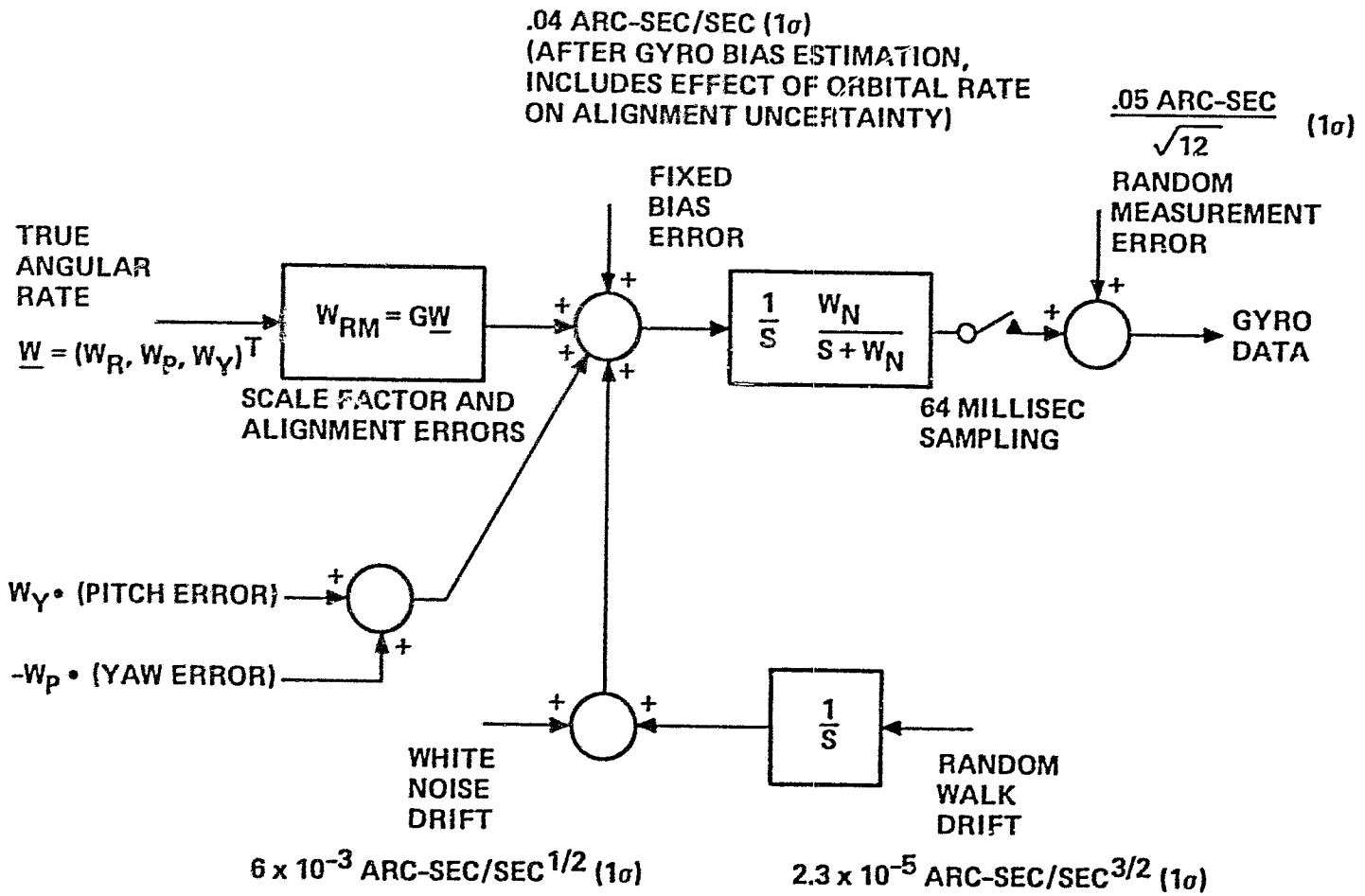

[ONLY ROLL AXIS MODEL SHOWN]

W_R, W_P, W_Y: ROLL, PITCH YAW ANGULAR RATES

Under orbital conditions, a dynamic alignment error is expected to result from temperature variations within the spacecraft structure. The dominant source of these temperature variations is the operation of TM, MSS, Wideband Communications Subsystem and Multimission Spacecraft Modules. The thermal alignment rate error can be expected to be as large as 0.167 arc-sec/second (1σ) and this error effect will be removed by control point processing (Section 3.2). Figure 2-6 shows a typical alignment error model which has been used to evaluate the effects on ground processing.

FIGURE 2-6

SPACECRAFT ALIGNMENT DYNAMICS
(ACS TO TM OPTICAL AXIS)

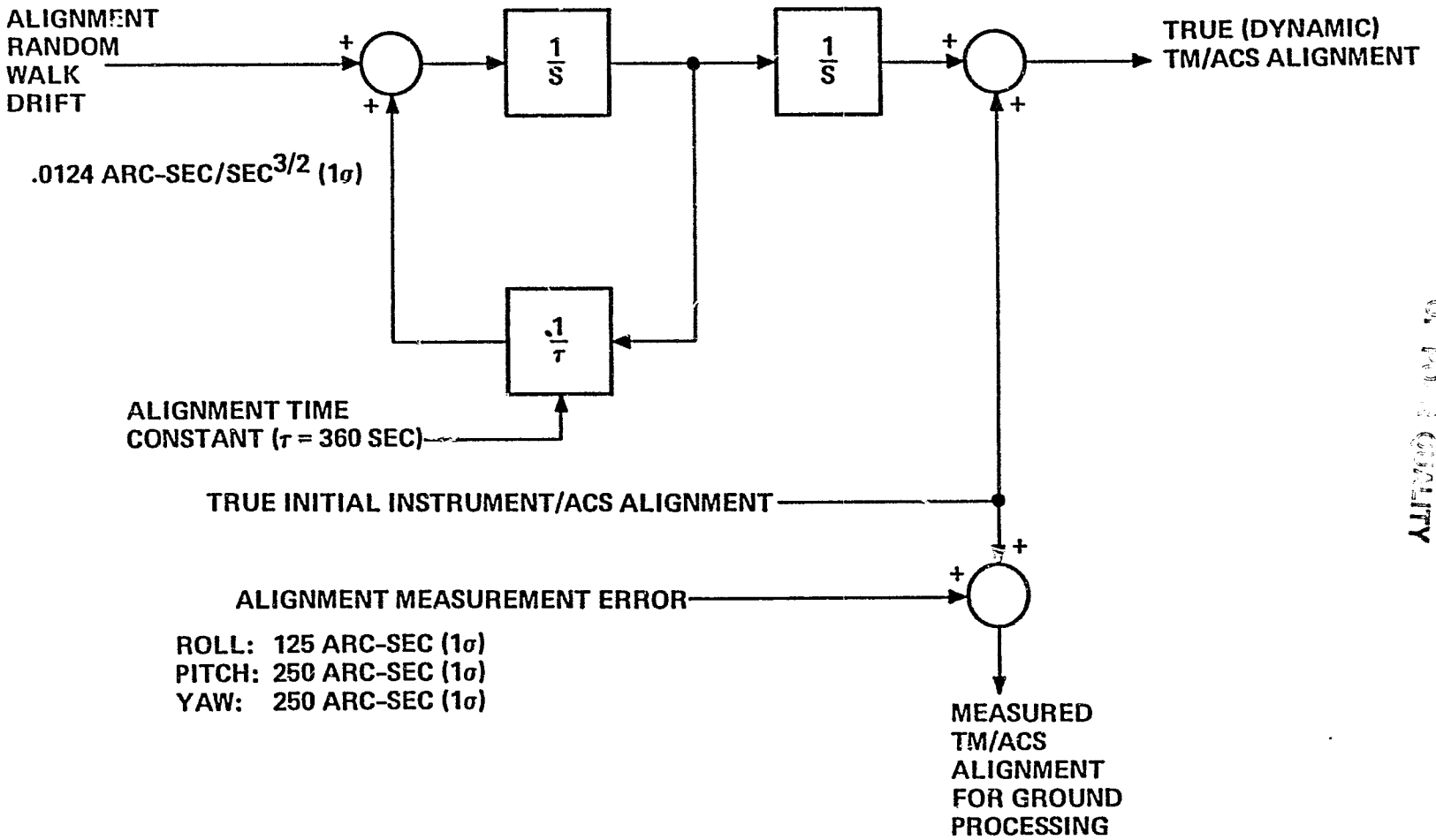

ACS: ATTITUDE CONTROL SYSTEM

High Frequency Attitude Disturbances

There are four dominant sources of high frequency (greater than 0.01 Hz) mechanical disturbances: TDRSS Antenna drive, solar array drives, MSS scan mirror, and TM scan mirror. Interaction of these disturbances with the spacecraft structure causes attitude deviations. An extensive effort involving structural testing, modeling and simulation analysis characterized these interactions. A brief summary of these results will be given.

The TDRSS antenna is driven around the spacecraft z-axis (azimuth) and an elevation axis to follow the relative motions between Landsat-D and the earth synchronous TDRSS. A stepper motor drives the antenna. Under normal operating conditions, there are between 0 and 3 steps per second required to exactly follow TDRSS in elevation. The rate depends upon the relative position between Landsat-D and TDRSS. A randomizing antenna control system is implemented in the on-board computer that avoids dwelling on large structural resonances in the 0-3 Hz frequency region.

The solar array is driven open loop to follow the sun by a stepper motor (19.66 steps/second). The resultant spacecraft disturbance is estimated to be 0.2 arc-second (RMS). When the solar array position is adjusted to compensate for misalignment with the sun, much larger disturbances will occur. Solar array adjustment will not occur immediately before or during TM instrument operation.

Figure 2.7 shows simulation results of a typical 30 second running RMS of spacecraft attitude deviation (above 0.01 Hz) which results from TDRSS Antenna and solar array operation. Under worst case conditions, the RMS excitation (over 30 seconds) may approach 10 arc-seconds in the bandwidth 0.01 to 0.4 Hz, but is expected to be less than 0.3 arc-second above 0.4 Hz.

FIGURE 2-7

TYPICAL TDRSS AND SOLAR ARRAY INDUCED ATTITUDE DEVIATION
(RUNNING 30 SECONDS RMS ABOVE 0.01 Hz)
TDRSS AT 30 DEG.

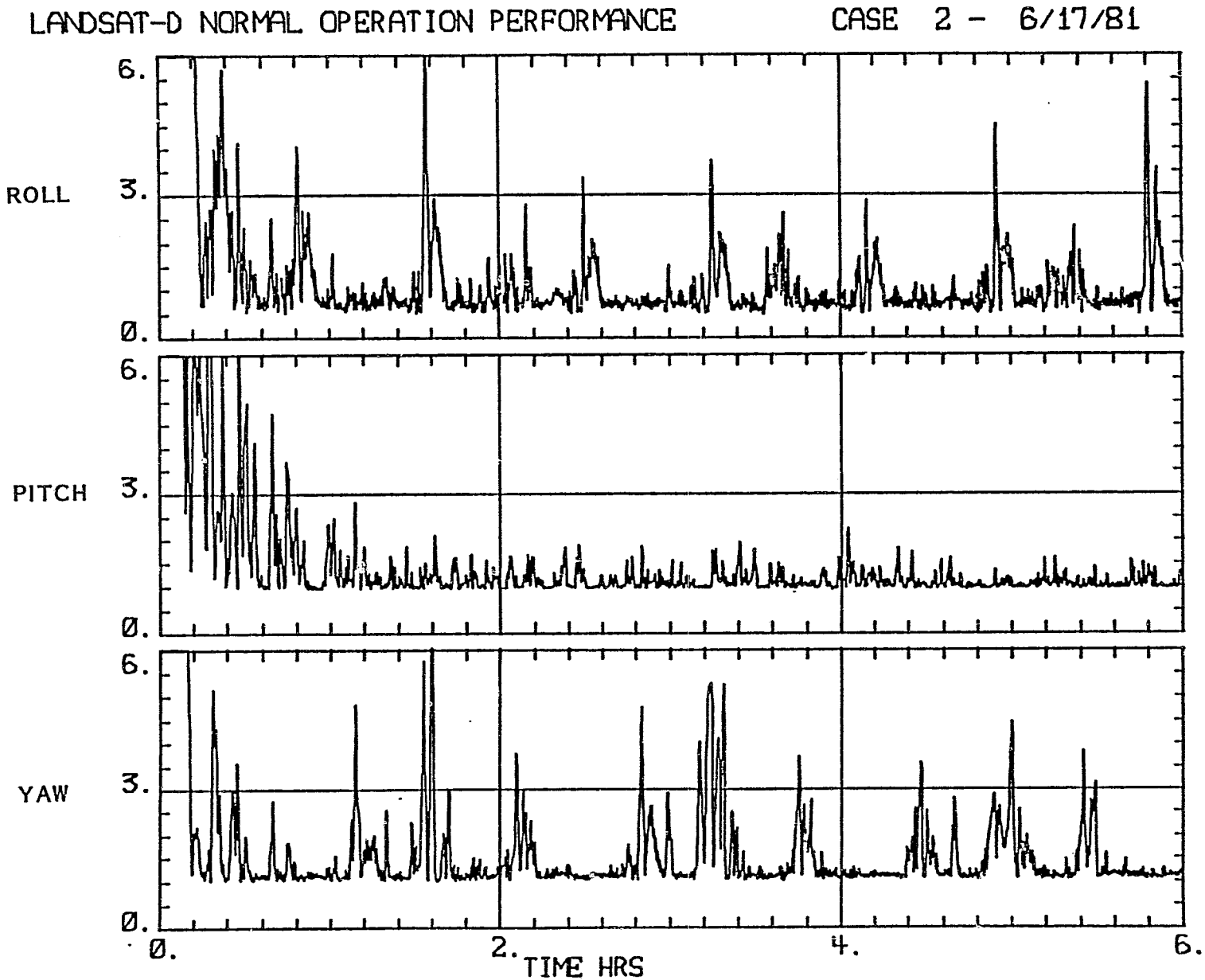

The low level of attitude deviation due to the TDRSS antenna has been achieved through design of their control systems. No such control could be exercised for the TM and MSS instruments. The bumper impacts of the MSS and TM scan mirrors will create attitude deviations. MSS and TM scan mirrors operate at 13.62 and approximately 7 Hz respectively. The alternating direction and impulsive impact of the scan mirrors produce significant torque amplitudes at odd harmonics (see Table 2-1). Structural analysis has shown that the frequencies of concern are 7 and 63 Hz for TM excitation and 68.1 Hz for MSS exciting TM. Based on test verified structural models, the roll, pitch, yaw attitude deviations due to the TM scan mirror are predicted to be 0.9, 0.2 and 0.3 arc-second (RMS), respectively. However, within the uncertainty of the structural modeling process, significantly higher amplitudes can be encountered. The ground processing is designed to meet temporal registration specifications with roll, pitch and yaw attitude deviations of 20.0, 2.2 and 16.3 arc-seconds, respectively.

High Frequency Attitude Measurements

The high frequency attitude disturbances cannot be reduced to an acceptable level through structural design. Recall in Section 1.2 it was shown that 1.13 arc-second (1σ) constituted the entire temporal registration error budget for a single scene. The actual allocation to high frequency attitude error is 0.5 arc-second (1σ). This situation forced Landsat-D to measure the attitude deviations of the spacecraft and to provide a companion correction capability in the ground processing. After consideration of available measurement devices, structural flexibility, and accuracy, size and power requirements, it was decided to use a combination of the existing ACS gyro package (DRIRU) and a small three axis Angular Displacement Sensor Assembly (ADSA) to measure TM attitude deviations. The DRIRU measures angular displacements in the 0 to 2 Hz band and the ADSA measures angular displacements in the 2 to 125 Hz band. Their data is combined in ground processing (see Section 3.1)

TABLE 2-1

AMPLITUDES OF TM AND MSS SCAN MIRROR TORQUE COMPONENTS

TM		MSS	
FREQUENCY (Hz)	AMPLITUDE (IN-LBS)	FREQUENCY (Hz)	AMPLITUDE (IN-LBS)
7	43.343	13.620	40.398
21	41.543	40.860	39.507
35	39.106	68.100	37.770
49	33.341	95.340	35.269
63	27.663	122.580	32.122
77	21.547	149.820	28.476
91	15.476	177.060	24.494
105	9.8845	204.300	20.351
119	5.1200	231.540	16.217
		258.780	12.253
		286.020	8.601
		313.260	5.373
		340.50	2.651

to yield angular displacements in the 0 to 125 Hz band.

The DRIRU is a NASA Standard. It contains 3 two-degree-of-freedom dry tuned gyros operating in a strapdown mode. The gyros are oriented such that redundant measurements are provided along three orthogonal axes. The output of each gyro channel is an asynchronous pulse train in which each pulse represents an incremental angular rotation about the gyro input axis. The pulses are accumulated in a register which is sampled every 0.064 seconds by the on-board computer. The key DRIRU performance parameters per axis are:

Drift Rate: 0.05 arc-second/second (1σ)
Drift Rate Stability: 0.003 arc-second/second (1σ) over 6 hours of operation
Noise: 1 arc-second (0 to peak) after linear drift removal
Bandwidth (3 dB): between 1.5 and 2.5 Hz
Quantization: 0.05 arc-second/pulse
Sample Time: 0.064 second

The Angular Displacement Sensor Assembly consists of three independent angular displacement sensors (ADS) oriented along orthogonal axes. As shown in Figure 2-8, the ADS uses a fluid-rotor inertia element which stands still in space as the case is oscillated about its input axis. A vane assembly is immersed in the fluid and its position with respect to the case is sensed with a low noise dual inductive pickoff. The pickoff system produces an analog signal output which is directly proportioned to the deviation of the vane assembly from its null position. To maintain the vane assembly at the desired null position an electrical auto-null system is used to feed back a torque to the moving vane assembly. The feedback is in part proportional to the integral of the output signal, keeping the average vane position at a fixed output value. This in turn keeps the vane assembly average position at the null position of the pick-off and the ADS does not respond to any

FIGURE 2-8

ANGULAR DISPLACEMENT SENSOR

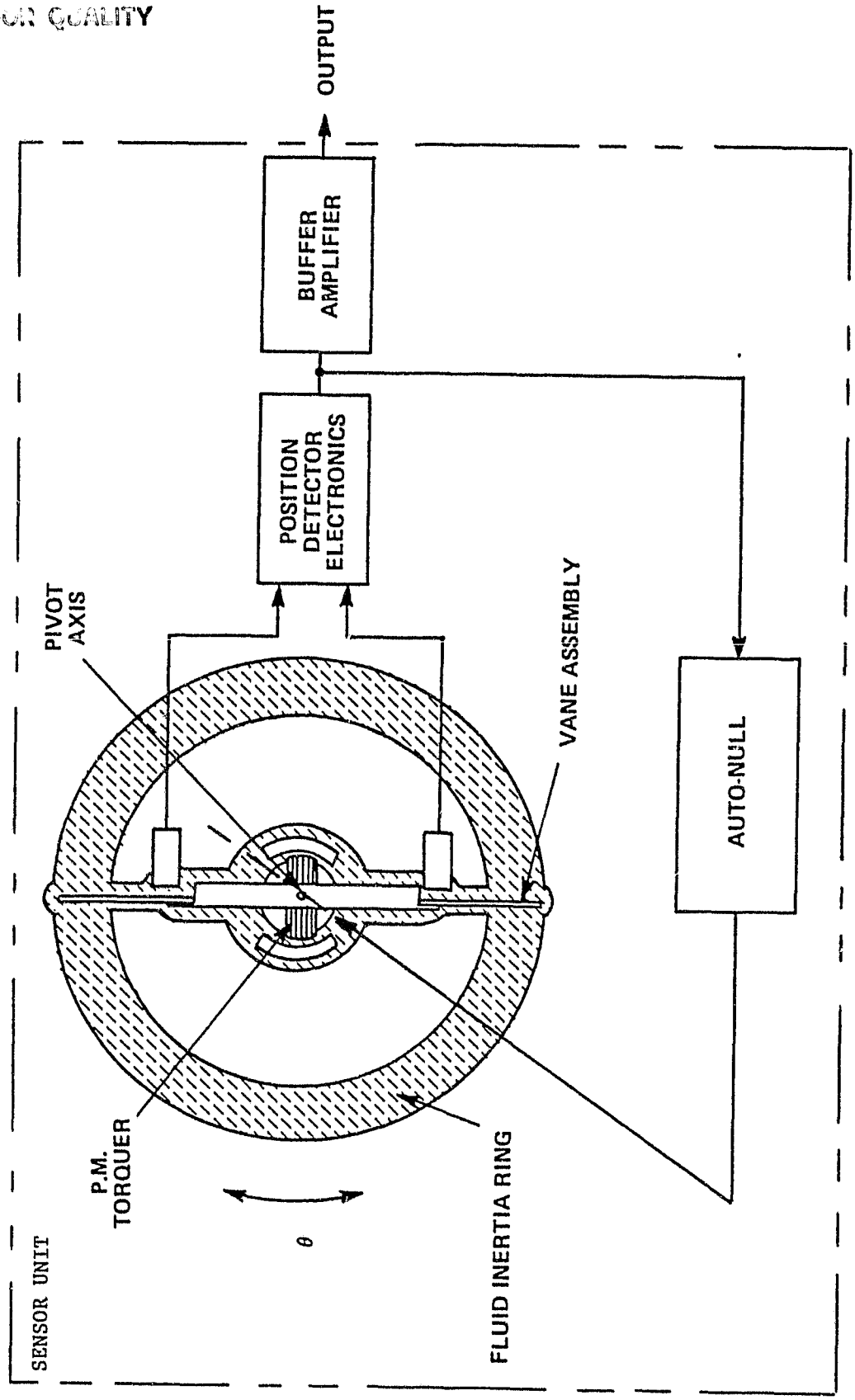

low frequency inputs. Since the auto-zero feedback loop contributes torque proportional to position as well as the integral of position, it produces a low natural frequency second-order system response in combination with the inertia of the rotor, with a nominal loop closure at 2 Hz. This provides an overall amplitude frequency response for the unit which rises at 18 dB/octave to 0.05 Hz, at 12 dB/octave from 0.05 to 2 Hz and is nominally flat from 2 Hz to 2000 Hz. Significant phase shift exists below 30 Hz.

Three ADS sensors are mounted in the ADSA along with presample low pass filter and A/D electronics. Key ADSA performance parameters per axis are:

Noise: 0.01 microradian (RMS)
Bandwidth (3 dB): 2 to 125 Hz (nominal)
Threshold: Not measurable
Quantization: .25 microradian (nominal)
Full scale reading: 250 microradians
Sample time: 0.002 seconds

2.3 Thematic Mapper

TM Geometric characteristics have impacts on the ground processing. While the TM and MSS both employ object plane scanning, certain TM geometric characteristics differentiate the two instruments. In general, these characteristics are related to the TM bidirectional scanning, the relatively wide focal place separation of TM spectral bands, the decreased TM field-of-view size, and the availability of good performance data. A brief review of significant TM geometric characteristics follows.

Focal Plane Layout and Detector Sampling

A geometric overview of TM is shown in Figure 2-9. The TM detectors are arranged in two focal plane assemblies: primary and cold. The primary focal plane assembly (PFPA) consists of four high resolution spectral bands each having 16 detectors, and an instantaneous field-of-view (IFOV) of 42.5 microradians. The odd numbered detectors are arranged in a row normal to the scan direction. The even detectors are arranged in a parallel row, offset 1 IFOV in the cross scan direction and 2.5 IFOV's in the along scan direction. The cold focal plane assembly (CFPA) consists of two high resolution bands each of which is arranged similarly to the high resolution bands of the PFPA. The cold focal plane assembly also consists of a thermal band which has only four detectors with a 170 microradian IFOV. Figure 2-10 shows the overall layout of the focal plane assemblies with the cold focal plane projected to the prime focal plane location.

The detector arrays are swept back-and-forth approximately normal to the ground track by the scan mirror. A West-to-East scan (on a daytime descending orbit pass) is called a forward scan. The East-to-West scan is called a reverse scan. Each high resolution band detector is sampled every 9.611 microseconds which corresponds to

FIGURE 2-9

THEMATIC MAPPER GEOMETRY

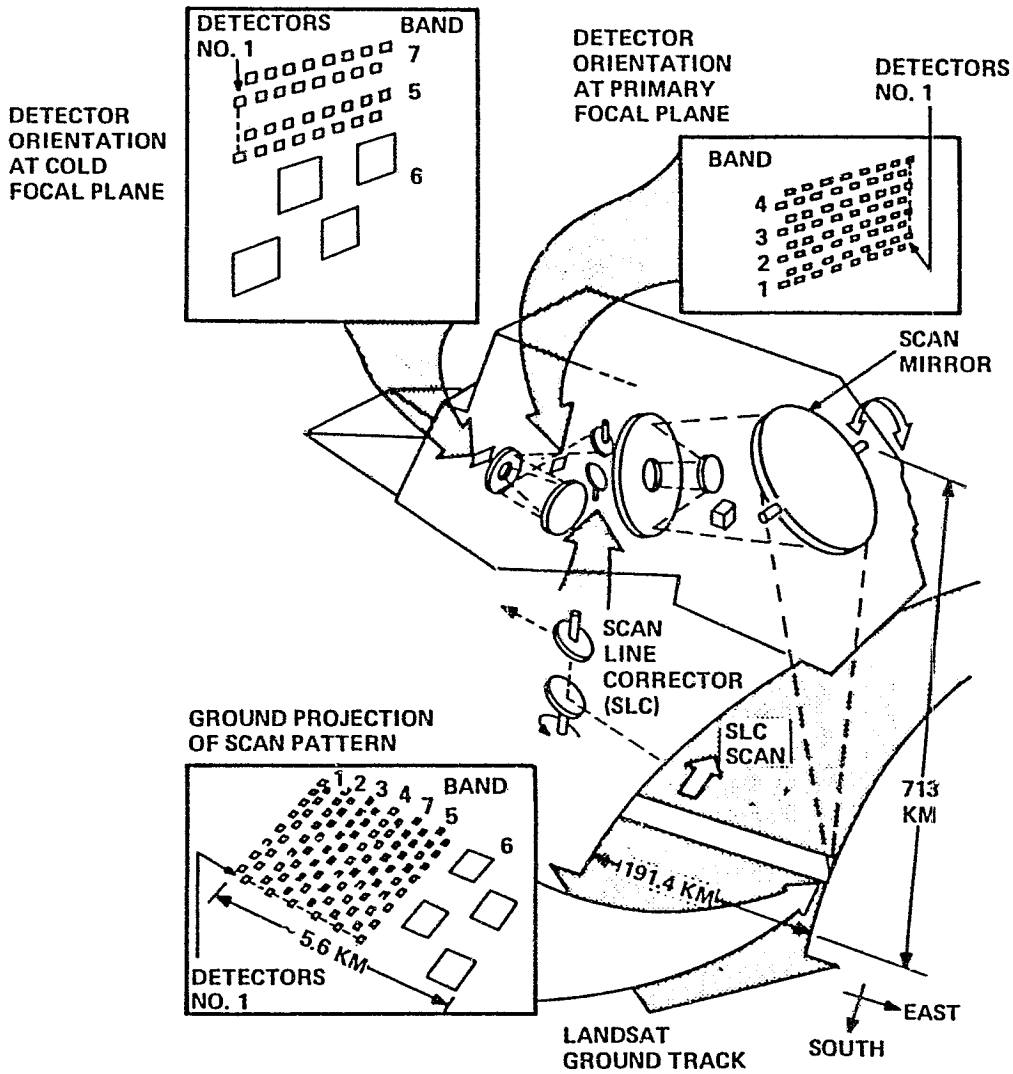

KEY GEOMETRIC FEATURES

- SCAN MIRROR
  - BI-DIRECTIONAL CROSS TRACK SCANNING
  - DATA AVAILABLE TO GROUND:
    - SCAN START TIME
    - SCAN DIRECTION
    - FIRST HALF SCAN TIME ERROR
    - SECOND HALF SCAN TIME ERROR
- SCAN LINE CORRECTOR
  - PROVIDES IN TRACK SCANNING
- TWO FOCAL PLANE ASSEMBLIES
- INSTANTANEOUS FIELD OF VIEW (IFOV)
  - BANDS 1-5, 7: 42.5 μrad (30 METERS)
  - BAND 6: 170 μrad (120 METERS)

FIGURE 2-10

DETECTOR PROJECTION AT PRIME FOCAL PLANE

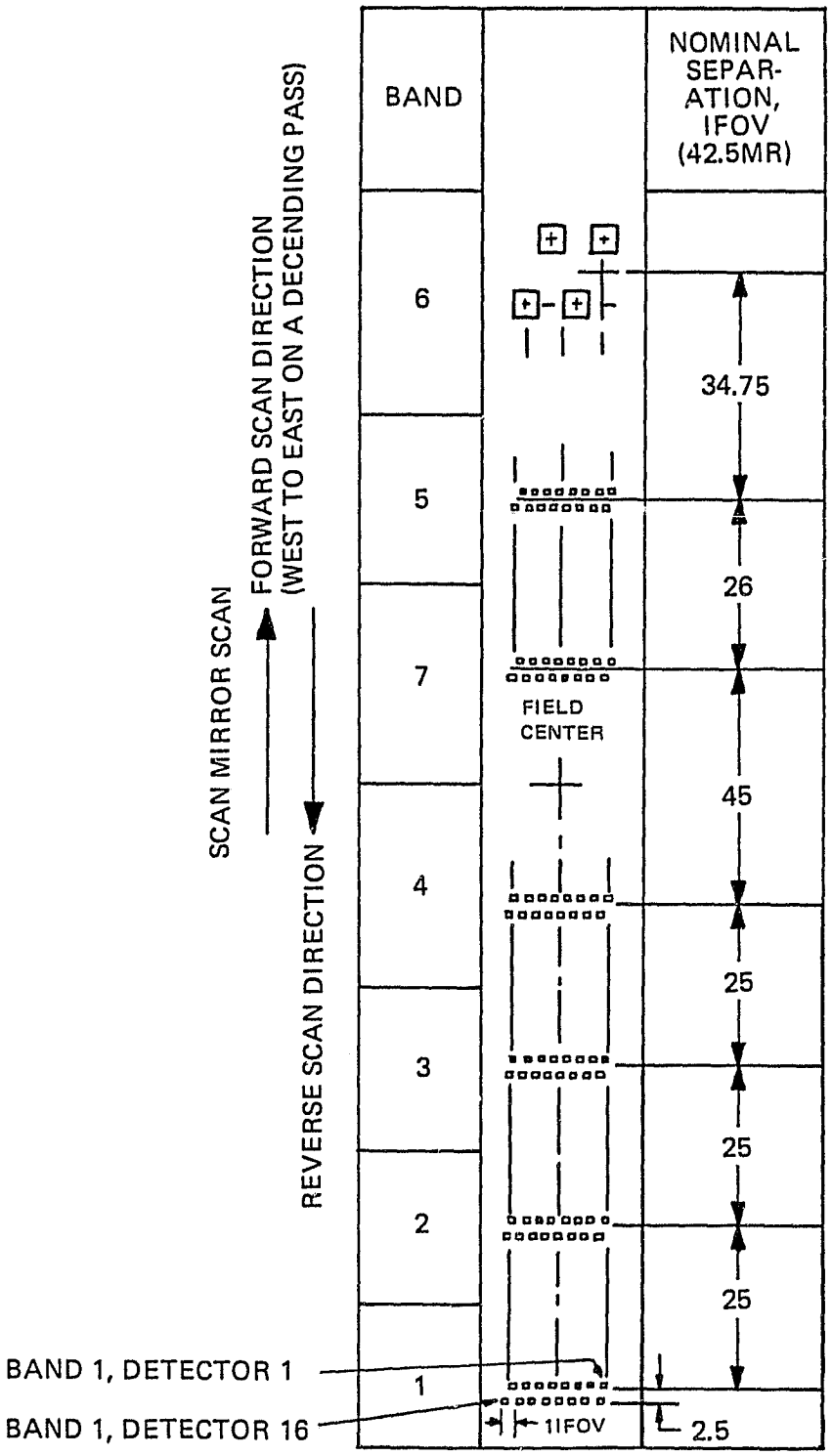

one IFOV (42.5 microradians) of nominal object space mirror motion. All odd numbered detector outputs are held at one time and all even number detector outputs are held one half sample time later. With the nominal 2.5 IFOV spacing between odd and even numbered detectors, this creates a 2 IFOV odd to even detector spacing on forward scans and a 3 IFOV spacing on reverse scans.

Scanning Mechanisms

The TM has two scanning mirrors: the Scan Mirror and the Scan Line Corrector. The Scan Mirror rotates about (approximately) the spacecraft x-axis and thus scans the detector arrays normal to the direction of flight. The scan mirror scan cycle is 7 $\pm$ .01 Hz. Nominally, the active scan time (imaging time) in one direction is 0.060743 seconds with 0.010719 seconds of turnaround time. The forward scan start and end are marked relative to the TM frame by an optical sensor called the Scan Angle Monitor (SAM). The SAM similarly marks the reverse scan start and end, with nominal co-location between forward scan start and reverse scan end and between forward scan end and reverse scan start. The SAM also identifies scan mirror mid-scan position.

The scan line corrector (SLC) scans about the spacecraft y-axis and sweeps the detector arrays to oppose the spacecraft ground track motion during the active portion of the scan. The SLC is reset during the forward and reverse scan mirror turnarounds. This generates an approximately parallel forward and reverse scan pattern on the earth.

Ideal TM scanning is illustrated in Figure 2.11. The 16 X 42.5 = 680 microradian wide band arrays are swept across the spacecraft ground track by the scan mirror. The increase in array ground width from the scan center to the extreme scan positions is a 5 meter "bow-tie" effect. The SLC scans against the along-track ground velocity

FIGURE 2-11
THEMATIC MAPPER SCANNING

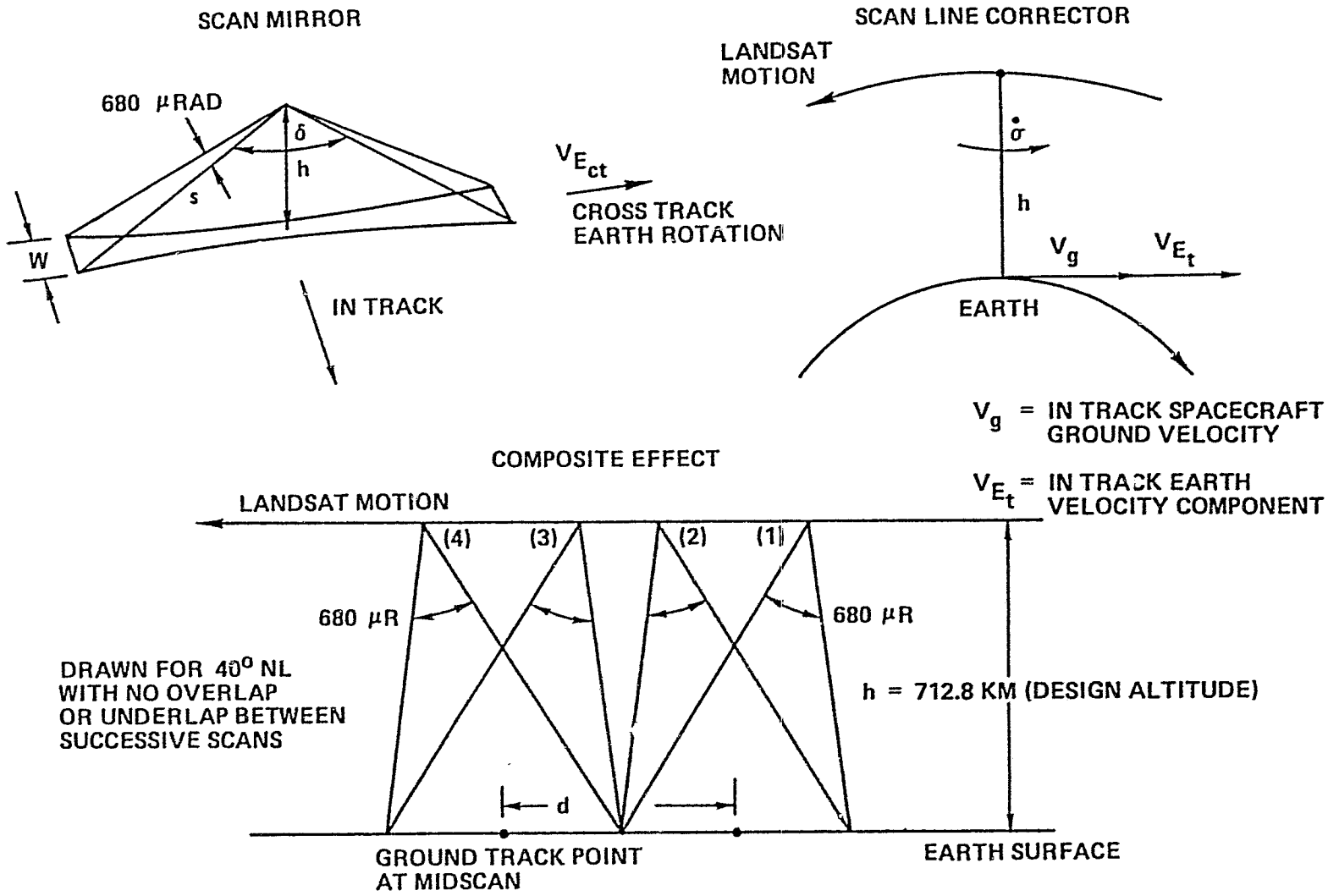

at a fixed rate which will cancel the in track earth velocity and the small in track earth rotational velocity component at the 712.8 km design altitude. The composite scan is illustrated in the lower part of Figure 2.11. At spacecraft position (1), the scan mirror is in its start scan position for a forward scan, and the SLC points the 680 microradian band arrays ahead of the sub-satellite point. The scan mirror moves the band arrays normal to the paper's plane, for nominally 0.060743 seconds, until the end of forward scan is reached. During that time, imagery is acquired, the spacecraft advances along its orbit, the SLC pushes the scan back along the ground track and the band arrays scanned normal to the ground track. At the end of forward scan (spacecraft position (2)), the SLC reset command is issued. During the nominal .010719 second scan mirror turnaround, the SLC is reset to its initial pointing angle, the spacecraft advances to position (3) and the scan mirror has moved to the start of reverse scan. The process is then repeated for the reverse scan.

The TM band array width, active scan time, scan mirror turnaround time and SLC active scan rates are fixed. They have been designed for an altitude of 712.8 km and an effective ground velocity of 6.821 km/second (the nominal condition at 40° Latitude) with the effect of bow-tie split,creating an equally small scan gap at scan center and overlap at scan end. However, spacecraft altitude varies between 696 and 741 km while velocity variations are small. As shown in Figure 2-12 at altitudes above the TM design point the scan width widens causing scan overlap and the SLC over-compensates the spacecraft ground track velocity causing scan skew. The actual scan error pattern is a composite of scan overlap, scan skew and bow-tie effects. The result is that the 16 detectors within a scan are always evenly spaced but the detector spacing between scans varies. The difference in ground spacing for detector spacing within a scan and for detectors 1 and 16 of two consecutive scans is called scan gap. Scan gap is positive when the spacing between scans is

FIGURE 2-12

THEMATIC MAPPER SCAN IS AFFECTED BY ALTITUDE DEVIATION

- OVERLAP BETWEEN SCANS

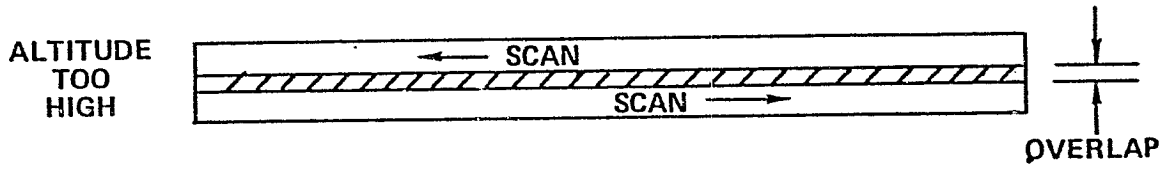

- SCAN SKEW

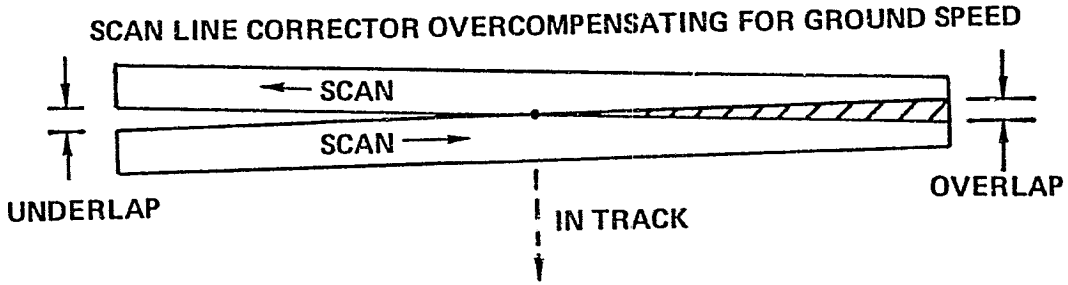

- BOW TIE EFFECT

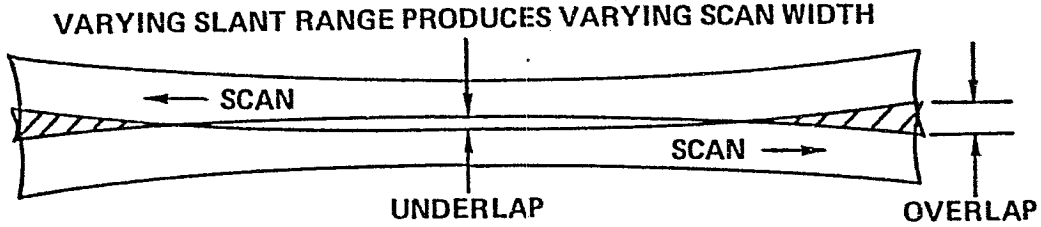

greater than the spacing within a scan. In general, scan gap varies across the scan and is usually greatest at the end of scans. Figure 2-13 shows the worst case end scan gap from altitude variation (as a function of Latitude), spacecraft attitude deviation, and TM overlap/underlap. The composite worst case range of scan gap is -2.8 IFOV to 2.0 IFOV. The altitude deviation scan gap error results from scan width, SLC skew and bow-tie effects. Spacecraft attitude deviation is caused by pitch and yaw axis motions and the one IFOV scan gap is a spacecraft structural design requirement. The TM underlap/overlap is the specified limit imposed on the instrument. It is expected that the attitude deviation effects will be substantially less than shown and that scan gaps due to altitude variation will dominate.

Scan Profiles

Ideally, the scan mirror has a constant angular rate over the active scan time (from scan start to scan end). As Figure 2-14 indicates, small rate variations will occur in scan mirror motion. The deviation in angular position from linear motion is called nonlinearity or profile. The profile results from small torques acting on the scan mirror. Magnetic compensators have been incorporated into the TM design that have the effect of significantly reducing the residual flex pivot torque. This results in an extremely linear mirror motion with worst case nonlinearity less than 200 microradians (object space). This low nonlinearity is required for good instrument level band-to-band registration due to the relatively wide geometric spacing between band arrays. It has been shown that the profile can be described by a fifth order polynomial and that different polynomials are required for forward and reverse scans.

After extensive scan mirror unit level testing, it was learned that the scan mirror profiles were not stable over time. They slowly "wander" about $\pm$ 20 microradians

FIGURE 2-13
SCAN GAP** ERROR

ALTITUDE VARIATION	SPACECRAFT ATTITUDE DEVIATION	TM UNDERLAP/OVERLAP
696 – 741 KM FOR 705.3 ORBIT 713 KM TM DESIGN ALTITUDE	LESS THAN 1 PIXEL	0.2 PIXEL (SPEC)

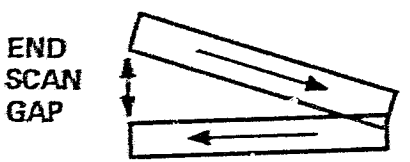

EARTH LOCATION	WORST CASE END SCAN GAP IN PIXELS*
NORTHERN HEMISPHERE	-0.7 TO 0.8
45°N	-0.4 TO 0.6
EQUATOR	-0.2 TO 0.8
45°S	-0.9 TO 0.1
SOUTHERN HEMISPHERE	-1.6 TO 0.8

WORST CASE GAP RANGE

-2.8 TO 2.0

(WORST CASE TOTAL OF ALTITUDE VARIATION, JITTER, TM UNDERLAP/OVERLAP EFFECTS)

*INCLUDES SCAN WIDTH, SCAN LINE CORRECTOR SKEW AND BOWTIE EFFECTS

**GAP < 0 : OVERLAP
= 0 : NOMINAL
> 0 : UNDERLAP

FIGURE 2-14

TM SCAN MIRROR PROFILE

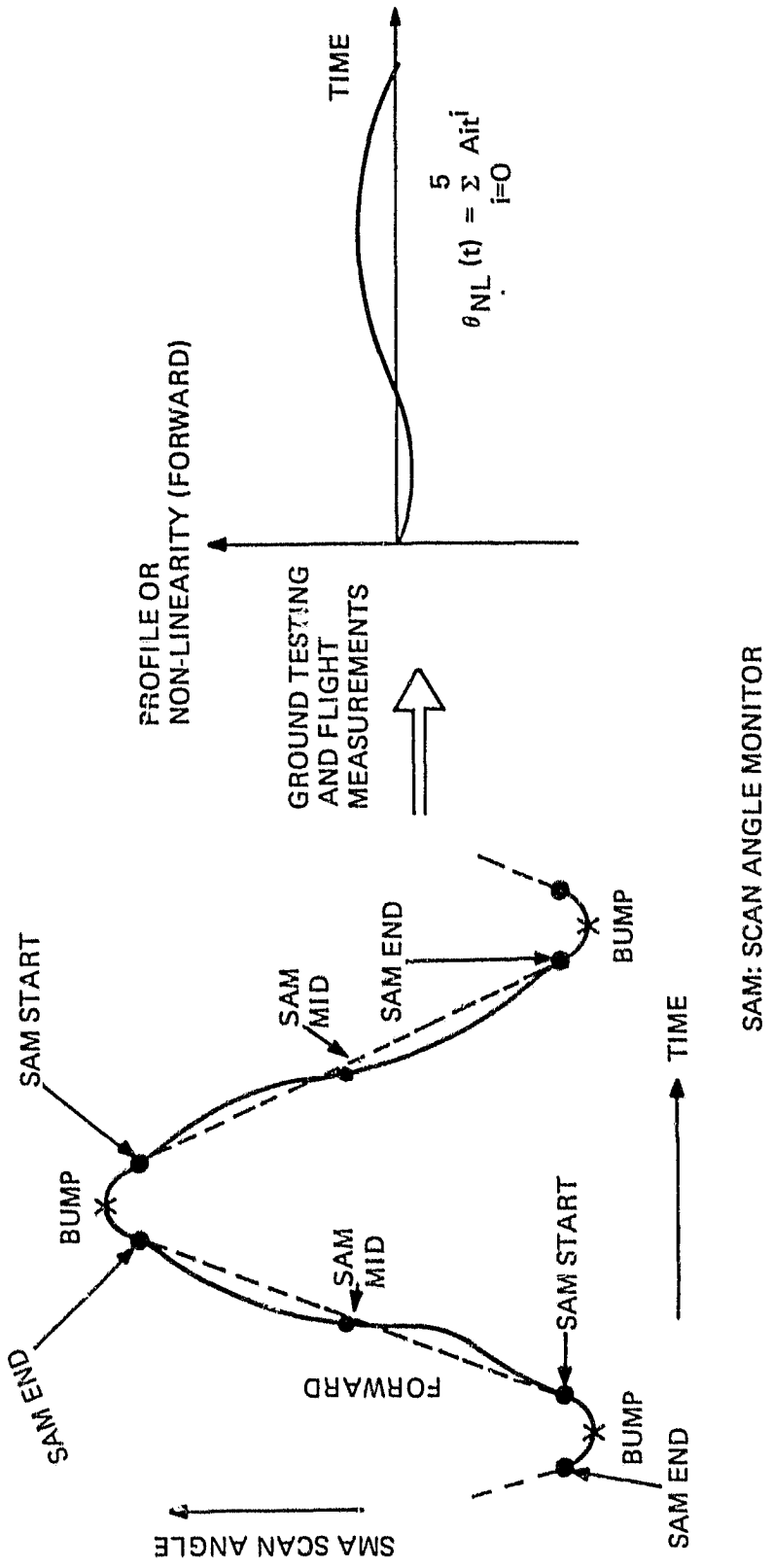

(object space) after days of operation. Wander is limited to the second order profile component and this can be estimated (see Section 3.1) by using information about first half scan and second half scan times. This data is supplied in the TM wideband data.

Nonlinearities in the cross axis scan mirror motion and in the SLC motions must also be compensated during ground processing.

Scan Line Length Control

Active scan time (the time from scan start to scan end) is also known as line length. The TM actively controls line length by measuring scan times and appropriately adjusting the torque magnitudes applied to the scan mirror during turnaround. The scan mirror is free running during the active scan time with no applied torque. This control scheme differs from that of the MSS which essentially controls scan cycle time (start to start time). The TM scan control is insensitive to attitude deviations which are self induced. Under such conditions, line length variations of 1 microsecond (1σ) are typical. However, it is extermely sensitive to externally induced attitude deviations. For example, one microradian of MSS excitation at 68.1 Hz is capable of creating line length variations of 16 microseconds or about 70 microradians in geometric effect. Line length variations as large as 400 microseconds are anticipated in ground processing design.

Forward to Reverse Scan Discontinuity

The bi-directional TM scanning introduces a number of significant factors that were not present with the MSS design. The different forward-to-reverse profiles have already been mentioned. Detector amplifier delays (typically 10 microseconds) and SAM electronic delays act in the opposite directions for the forward and reverse scans. The result is a forward to reverse scan discontinuity which must be corrected during ground processing.

2.4 Flight Segment Correction Data

There are two sources of Flight Segment data needed for geometric correction ground processing: Mirror Scan Correction Data (MSCD) and Payload Correction Data (PCD). The Mirror Scan Correction Data is imbedded into the TM wideband data. It includes the spacecraft time at scan start (scan time), the first half scan time error, the second half scan time error and the scan direction (forward or reverse) indicator. The scan time is the spacecraft time, with 0.0625 millisecond precision, at the scan mirror start position. This time is used to relate scan mirror position to the ephemeris, ADSA and DRIRU data. The time at any TM detector sample is obtained by adding 9.611 microseconds times the sample number to the scan time. The first half and second half scan time errors define the time error from a nominal scan time. These errors are known to a 0.188 microsecond precision and are determined from the TM oscillator.

Payload Correction Data includes ADSA angular samples every 0.002 seconds per axis, DRIRU output register samples every 0.064 seconds per axis, DRIRU drift estimates every 16.384 seconds per axis, ephemeris data every 8.192 seconds, spacecraft time, and TM housekeeping telemetry data. PCD is transmitted via a 32 kilobit/second telemetry link and is also imbedded into the TM wideband data. Figure 2-15 shows the PCD attitude data and scan start timing. All PCD data collection is driven by the spacecraft oscillator. This oscillator generates time code which identifies the TM start scan time and is imbedded into the PCD telemetry cycle. The spacecraft oscillator synchronizes ADSA sampling and synchronizes on-board computer (OBC) operation. The OBC executive scheduler in turn drives DRIRU sampling.

The ADSA samples and OBC Data are supplied to the PCD Formatter which constructs the PCD Telemetry Cycle Data. This is a fixed format telemetry data package occuring every 16.384 seconds. For each occurrance of a given data item in the

FIGURE 2-15
ATTITUDE DATA AND SCAN START TIMING

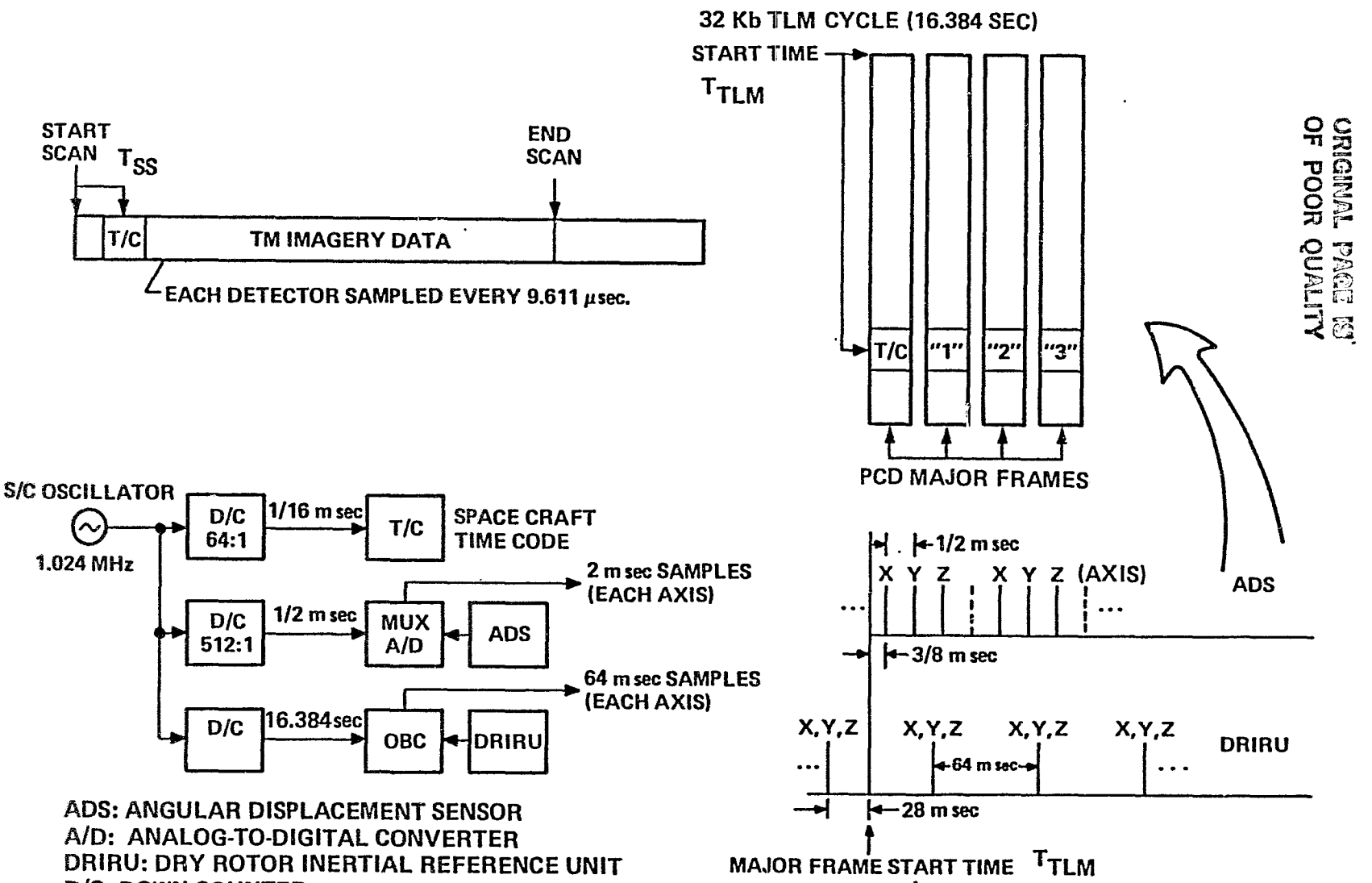

PCD telemetry cycle, its occurrence time relative to the imbedded time code is known. For example, as indicated in Figure 2-15, the first ADSA x-axis sample was taken 3/8 milliseconds after the telemetry time code and each subsequent x-axis sample in the PCD cycle occurs every 0.002 seconds.

III. GROUND SEGMENT

With respect to geometric correction, the Landsat-D Ground Segment uses Mirror Scan Correction Data, Payload Correction Data and control point information to determine where TM detector samples fall on output map projection systems. Then the raw imagery is reformatted and resampled to produce image samples on a selected output projection grid system.

Figure 1-4 is repeated here for convenience. It shows the TM geometric correction functions performed by the ground processing. These functions were briefly described in Section 1.0 and will now be discussed in more detail.

3.1 Payload Correction Processing

Payload Correction Processing uses Payload Correction Data (PCD) and Mirror Scan Correction Data (MSCD) to generate Systematic Correction Data (SCD). All subsequent processing uses the relatively simple SCD to determine TM imagery geometric distortions. SCD provides a means of locating TM detector samples on the output projection system. Large bias and relatively slowly varying drift errors are contained in the available attitude, ephemeris, time and TM alignment information used in generating the SCD. These errors remain in the SCD but their effect is removed during control point processing. A set of SCD applies to World Reference System scene and consists of four data groups: Benchmark Matricies, High Frequency Matricies, Focal Plane Geometry Matricies, and Processing Parameters.

Benchmark Matricies define the location of the TM optical axis assuming perfect attitude, linear scan mirror motions, linear SLC motions and nominal active scan

FIGURE 1-4

LANDSAT D TM GEOMETRIC CORRECTION SYSTEM OVERVIEW

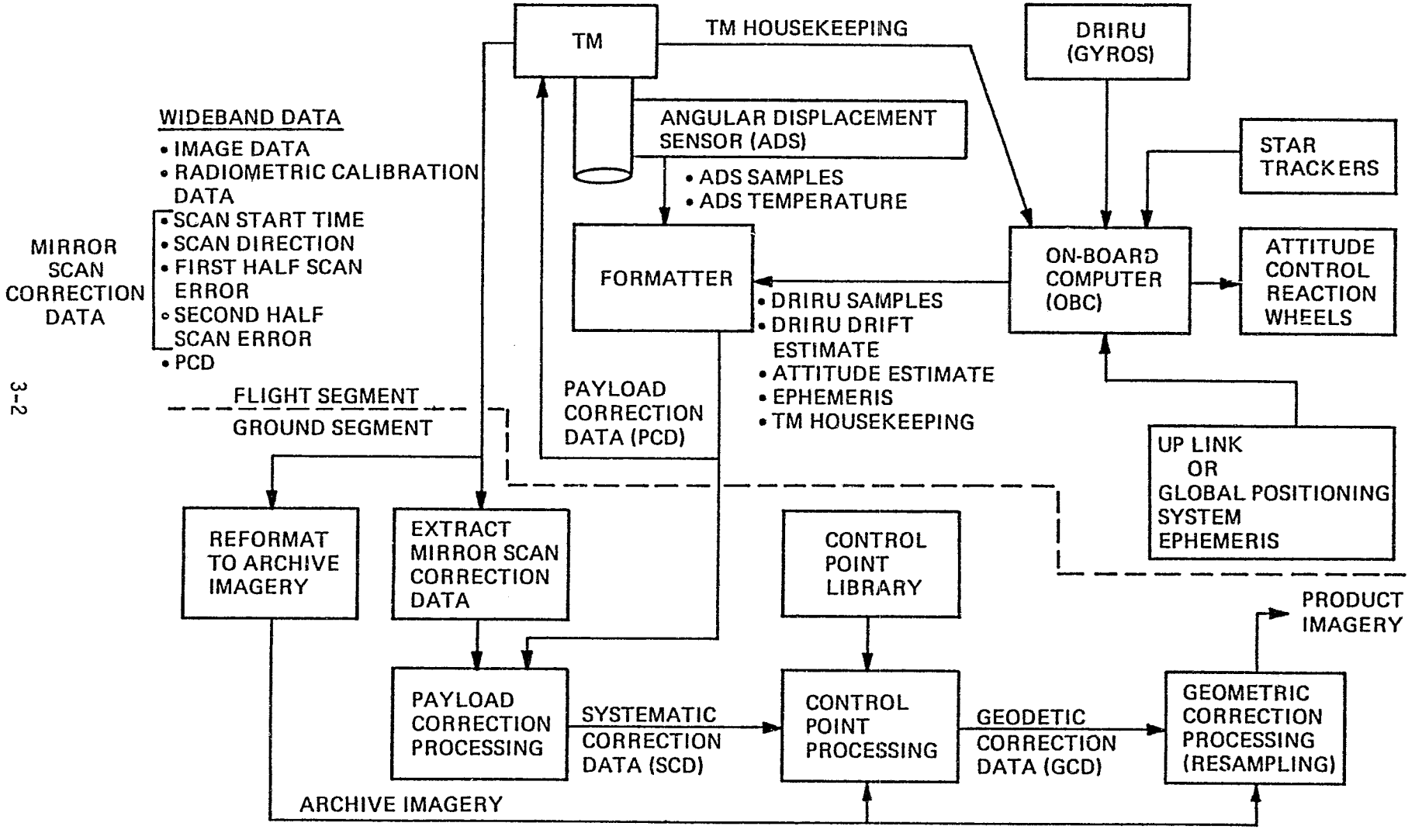

times. Ephemeris, TM alignment, actual scan start times and map projections are used in generating the Benchmark Matricies. These matricies include only slowly varying distortion information and thus are defined on a relatively sparce grid system consisting of 256 data items per WRS scene. Any given detector sample is located by interpolating the grids. The Benchmark Matricies provide the basic geometric distortion information. All other distortions resulting from attitude deviations, scan profiles or actual detector location on the focal plane assemblies are additive.

High Frequency Matricies define the attitude deviations, scan profiles and line length variations of each scan in the WRS scene. These matricies are time based and define the high frequency optical axis deviations from the Benchmark Matricies. This data is considerably more dense and consists of 26180 data items per WRS scene.

Focal Plane Geometry Matricies define the geometric adjustments needed to move from the optical axis location to that of any TM detector. These adjustments include actual focal plane detector location and the geometric effect of electronic time delays. The data quantity is relatively small consisting of 240 Data Items per WRS scene.

Processing parameters are data items, such as scan line length and detector offset adjustments made during image reformatting. They are needed during image resampling processing.

As shown in Figure 3-1, Payload Correction Processing consists of three major functions: Payload Correction Data Processing, Mirror Scan Correction Data Processing and Systematic Correction Data Generation.

FIGURE 3-1

PAYLOAD CORRECTION PROCESSING

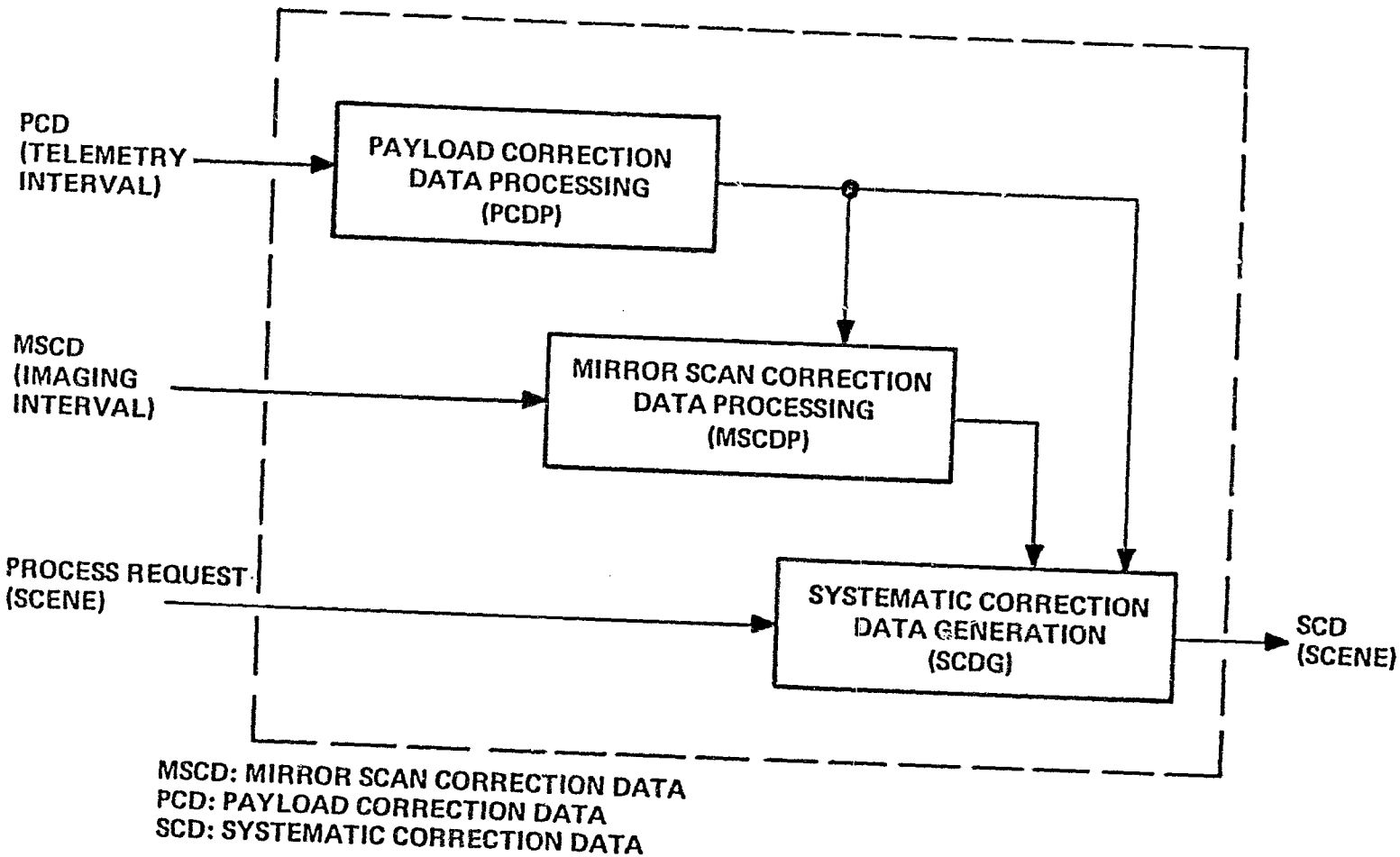

Payload Correction Data Processing

Payload Correction Data Processing operates on the ephemeris information and attitude deviation measurements (ADSA and DRIRU Data) from the spacecraft Payload Correction Data (PCD). This processing synchronizes all attitude and ephemeris data to a common PCD telemetry start time for ease of subsequent processing.

The ephemers data from PCD arrives as Earth Centered Inertial position and velocity estimates every 8.192 seconds. This received ephemeris is not directly suitable for precision image processing due to on-board computer processing errors, potential Global Positioning System data discontinuities and telemetry errors. The control point processing (Section 3.2) requires a smooth analytic ephemeris with known error dynamics. This is provided by fitting the initial conditions of a second zonal harmonic (J2) orbit model to the received ephemeris. The fit error is used as a data quality indicator for the received ephemeris data. Ephemeris processing uses the fitted initial conditions to synchronize the ephemeris data with the PCD telemetry start time and regenerates the smoothed ECI ephemeris data every 2.048 seconds using the J2 model.

Attitude Data Processing (ADP) combines and synchronizes the ADSA and DRIRU attitude deviation information to yield TM optical axis roll, pitch and yaw attitude deviations in a zero to 125 Hz bandwidth. ADS and DRIRU data are first processed to replace bad values and are logically extended through missing data that may occur due to telemetry link errors. Figure 3-2 shows the functions performed in ADP. The 0.002 second ADSA roll, pitch and yaw axis samples are converted to microradian units, and synchronized to the PCD telemetry start time with .002 second sample spacing. The coordinate axes are then rotated to align with the TM optical axis.

FIGURE 3-2

ATTITUDE DATA PROCESSING

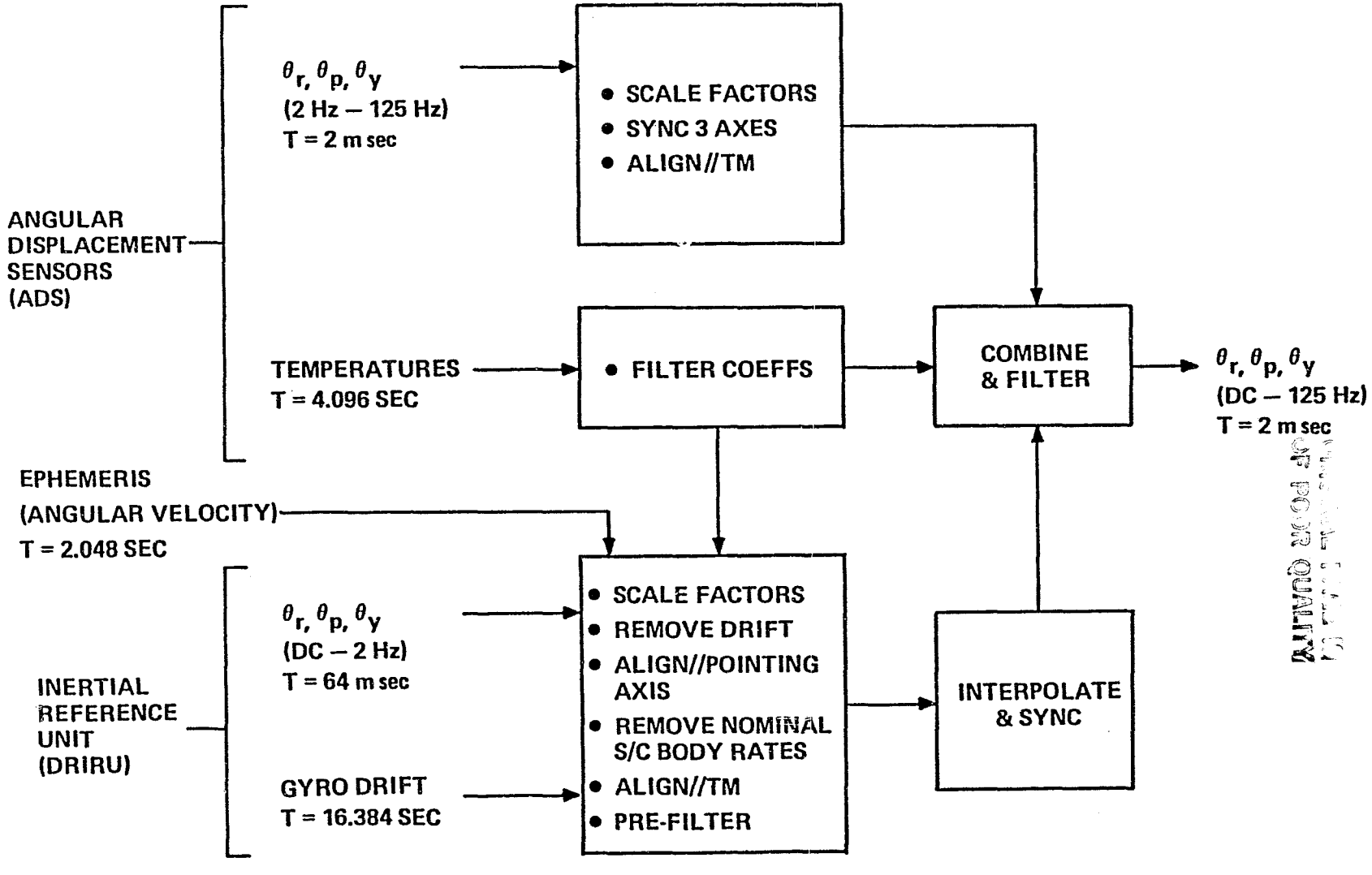

The 0.064 second roll, pitch and yaw DRIRU angles are similarly converted to micro-radian angular change units, the on-board computer gyro drift estimates are applied, the data is rotated to align with the spacecraft pointed axis, nominal body rates derived from ephemeris data are removed, the data is then aligned with the TM optical axis, and digitally pre-filtered. The processed DRIRU angular increments are then synchronized to the PCD telemetry start time and interpolated to 0.002 second samples.

The processed ADSA and DRIRU data are now in a common coordinate system and time synchronized. The data sets are then summed and digitally filtered to remove phase and amplitude distortions. The processing has been designed to provide less than 1% error.

Provisions have been made that allow modification of DRIRU pre-filter and final combined digital filter coefficients based on ADS temperature information. The need for this capability has not been demonstrated by ADSA testing and this filter coefficient processing is not being used.

Mirror Scan Correction Data Processing

Mirror Scan Correction Data Processing generates along scan profile deviations and cross scan profile deviations for each scan. The profile deviations are relative to the TM body axes and are time synchronized with the Attitude Data Processing outputs. The start scan times are also adjusted to use the PCD start time as their reference.

The Mirror Scan Correction Data (MSCD) Processing inputs (scan start time, first half scan time error, second half scan time error and scan direction) are imbedded by the TM into its wideband data. This data is extracted from the wideband data

and checked for self consistency. That is, proper scan time advancement, within tolerance variation in estimated nonlinearity at midscan, and scan direction changes are evaluated. Front end processing hardware also provides independent measures of total line length and start-scan to start-scan time. The number of 8 bit TM words between scan start and end codes imbedded in the TM wideband data are counted. Due to the critical need for proper MSCD, it is also checked for consistency against these independent measures. Errors are reported and best estimates are substituted for rejected MSCD values. The first half scan time errors and second half scan time errors are converted to mid-scan time interval and end-scan time interval for subsequent processing.

Figure 3-3 shows the MSCD Processing functional flow. Telemetry-Imagery Synchronization adjusts the scan start times to reference the PCD start time and computes the line length processing parameters needed during resampling. Scan Mirror Data Processing uses the relative scan start times, mid-scan interval time and end-scan time interval to interpolate the roll axis attitude deviations at scan start, mid-scan and end-scan times. These roll axis deviations along with the static first half and second half scan angles, and the mid-scan and end-scan interval times are used to estimate the second order scan mirror profile adjustment. Nominally, a sliding 400 scan average is used to estimate the profile adjustment for each scan. A linear correction factor, based on end-scan interval time, is then used to modify the adjusted profile and generate along scan profile deviations at the same times as the ADP output samples.

Scan Line Corrector Data Processing generates cross scan profile deviations which arise from the Scan Line Correction (SLC) profile and the cross-axis scan mirror profile. The SLC position is reset by the end-scan Scan Angle Monitor (SAM) position and it

FIGURE 3-3

MIRROR SCAN CORRECTION DATA PROCESSING

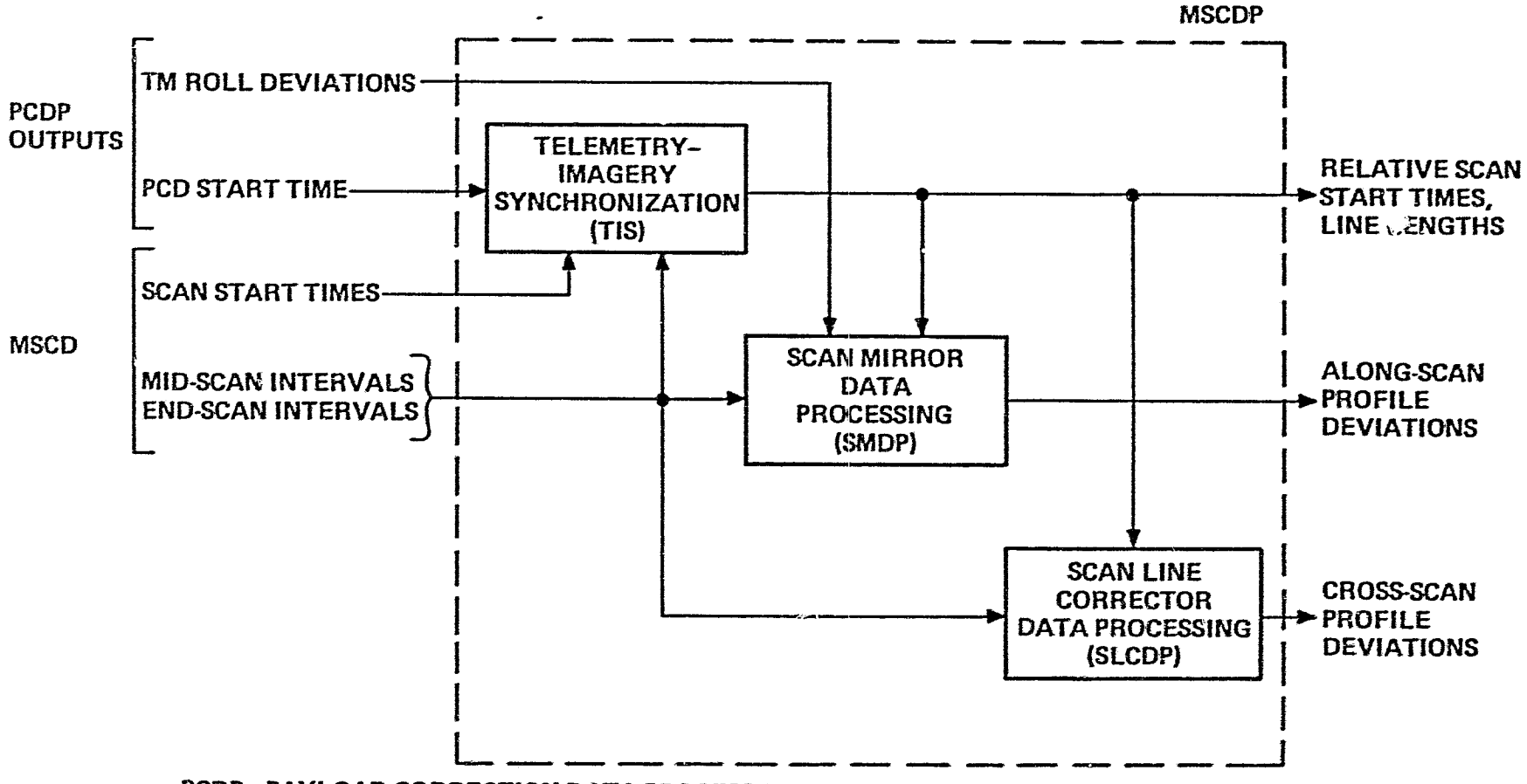

PCDP: PAYLOAD CORRECTION DATA PROCESSING
MSCD: MIRROR SCAN CORRECTION DATA PROCESSING

initiates active scanning independent of the SAM start. Thus, mirror turnaround variation effects the coordination between SLC and the scan mirror. The nominal SLC profile is, therefore, adjusted based upon mirror turnaround time. A linear correction factor, based on end-scan interval time, is also applied to adjust the cross-axis scan mirror profile. The composite adjusted cross-axis scan mirror and SLC profiles are then used to generate cross axis profile deviations at the same times as the ADP output samples.

Systematic Correction Data Generation

PCD Processing and MSCD Processing have both compensated and time synchronized the ephemeris, attitude deviation and scan profile data. The final function of Payload Correction Processing is Systematic Correction Data (SCD) Generation. Figure 3-4 shows the SCD Generation Processing flow. An overview of SCD content is shown in Figures 3-5, 6 and 7.

Image framing determines the WRS scene parameters. Scene center time, scene center scan, and output coordinate system scene center X-shift are determined from World Reference System path and row identification. The output projection scene center location is always X=0, Y=0 with output grid points spaced every 28.5 meters in X and Y.

The benchmark matrix calculation generates a grid of geometric distortion information for each output map projection. Figure 3-8 illustrates the benchmark matrix concept. This Figure shows an example of the optical axis path on a portion of the X,Y output coordinate system. The circles along the optical axis path represent sample times (every 9.611 microseconds) of odd numbered high resolution band detectors. The i value is the sample number relative to scan start. The benchmark value, P_0, indicates the fractional sample number and the benchmark value, Y_0, indicates the output projection Y coordinate where the optical axis path crosses a specific output projection X coordinate (X = 43.776 km for this example). The computation is also performed for a point on the focal plane shifted σ = 318.75 microradian cross-scan from the optical axis. These benchmark values are called P_1 and Y_1.

FIGURE 3-4
SYSTEMATIC CORRECTION DATA GENERATION

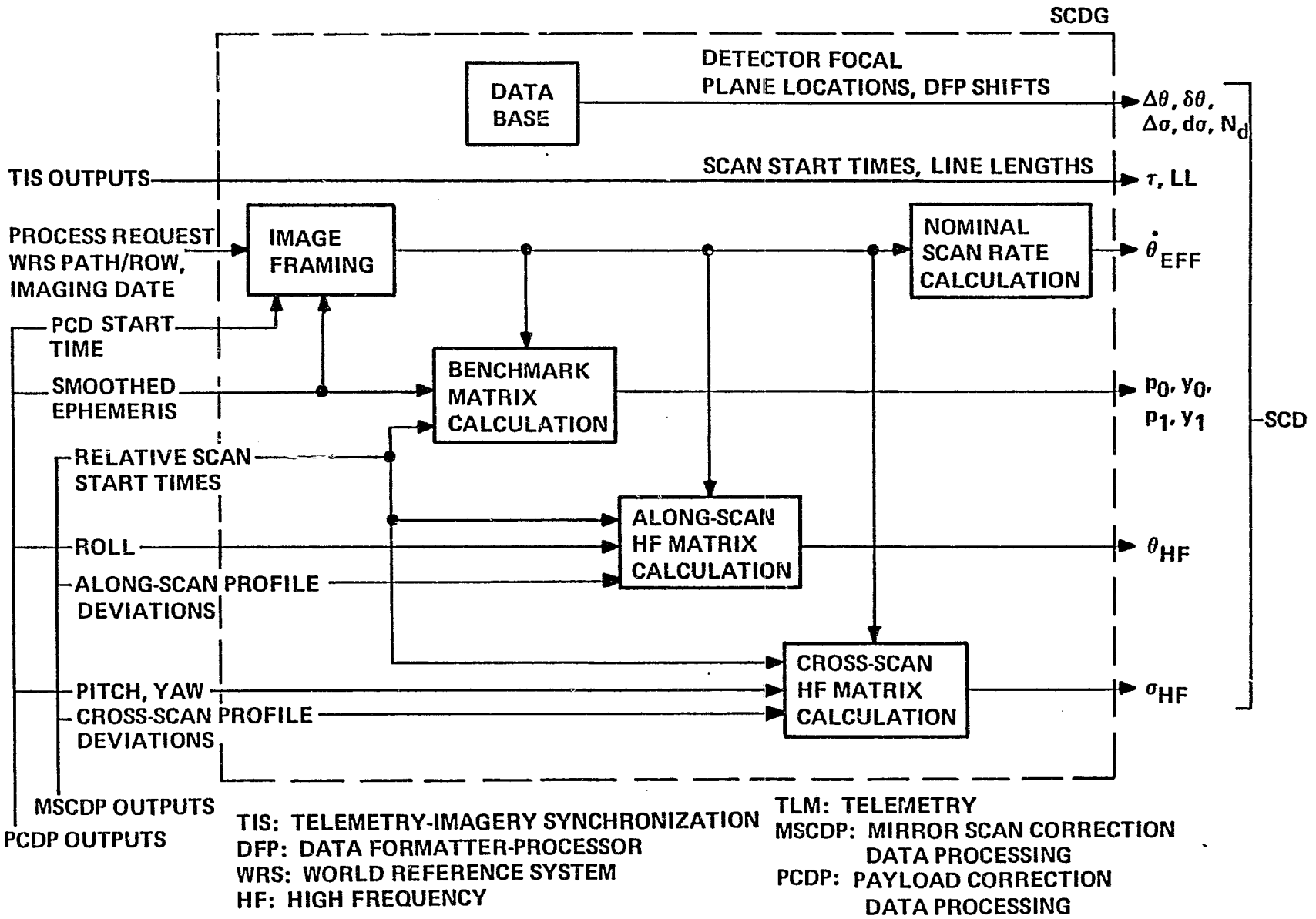

TIS: TELEMETRY-IMAGERY SYNCHRONIZATION
DFP: DATA FORMATTER-PROCESSOR
WRS: WORLD REFERENCE SYSTEM
HF: HIGH FREQUENCY

TLM: TELEMETRY
MSCDP: MIRROR SCAN CORRECTION DATA PROCESSING
PCDP: PAYLOAD CORRECTION DATA PROCESSING

FIGURE 3-5

SCD: OPTICAL AXIS POSITION ON THE OUTPUT COORDINATE SYSTEM

BENCHMARK MATRICES

p_0 (i,j,k), y_0 (i,j,k)

p_1 (i,j,k), y_1 (i,j,k)

i = x coordinate index = 1, . . . ,8

j = sweep index = 1, . . . ,4

k = scan direction index = 1,2

INCLUDES: EPHEMERIS, NOMINAL LINEAR TM ACTIVE SCAN, PERFECT ACS, KNOWN INSTRUMENT ALIGNMENT, MAP PROJECTION

(ONE SET FOR EACH PROJECTION)

ALONG SCAN

HIGH FREQUENCY MATRIX

θ_{HF} (i,j)

i = sample number index = 1, . . . ,35

j = scan number = 1, . . . ,374

INCLUDES: SMA ALONG SCAN PROFILE, SMA LINE LENGTH, S/C ROLL JITTER

MIRROR SCAN START TIMES

τ (j)

j = scan number = 1, . . ., 374

RELATIVE START TIME FOR EACH SCAN

CROSS SCAN

HIGH FREQUENCY MATRIX

σ_{HF} (i,j)

i = sample number index = 1, . . . ,35

j = scan number = 1, . . . ,374

INCLUDES: SMA CROSS SCAN PROFILE, SMA LINE LENGTH, SLC PROFILE, SLC DELAY, S/C PITCH AND YAW JITTER

SMA: SCAN MIRROR ASSEMBLY
SLC: SCAN LINE CORRECTOR
S/C: SPACECRAFT

FIGURE 3-6

SCD: OPTICAL AXIS TO DETECTOR SAMPLE LOCATION

NOMINAL POINTING VECTOR SCAN RATE ACROSS OUTPUT COORDINATES

$\dot{\theta}_{EFF}$ (k)

k = scan direction index = 1,2

NOMINAL ALONG SCAN FOCAL PLANE BAND LOCATION

$\Delta\theta$ (m)

m = band number = 1, . . . ,7

ALONG SCAN ANGULAR DISTANCE FROM OPTICAL AXIS TO BAND CENTER

NOMINAL CROSS-SCAN FOCAL PLANE BAND LOCATION

$\Delta\sigma$ (m)

m = band number = 1, . . . ,7

CROSS SCAN ANGULAR DISTANCE FROM OPTICAL AXIS TO BAND CENTER

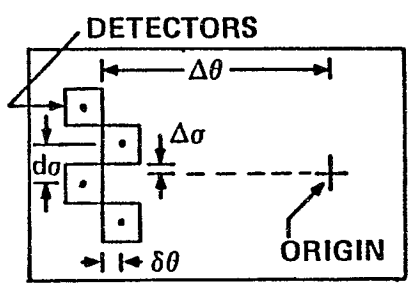

TM FOCAL PLANE

SAM: SCAN ANGLE MONITOR

ALONG SCAN FOCAL PLANE DETECTOR LOCATIONS

$\delta\theta$ (m,n,k)

m = band number = 1, . . . ,7

n = detector number = 1, . . . ,16

k = scan direction index = 1,2

INCLUDES: ALONG SCAN ANGULAR DISTANCE BETWEEN BAND CENTER AND DETECTOR LOCATION, DETECTOR CHANNEL DELAYS, SAM PULSE DELAYS

CROSS SCAN FOCAL PLANE DETECTOR SPACING

$d\sigma$ (m)

m = band number = 1, . . . ,7

AVERAGE INTER-DETECTOR CROSS SCAN FOCAL PLANE SPACING

FIGURE 3-7

SCD: PROCESSING PARAMETERS

SCAN LINE LENGTH

LL (j)

j = scan number = 1, . . . ,374

NUMBER OF COMPLETE IMAGING MINOR FRAMES

DATA FORMATTER – PROCESSOR ODD DETECTOR SAMPLE SHIFTS

N_d (m,k)

m = band number = 1, . . . ,7

k = scan direction index = 1,2

LINE SHIFT INTRODUCED BY THE DFP FOR ODD NUMBERED DETECTORS

FIGURE 3-8

BENCHMARK MATRIX CONCEPT
(AN EXAMPLE)

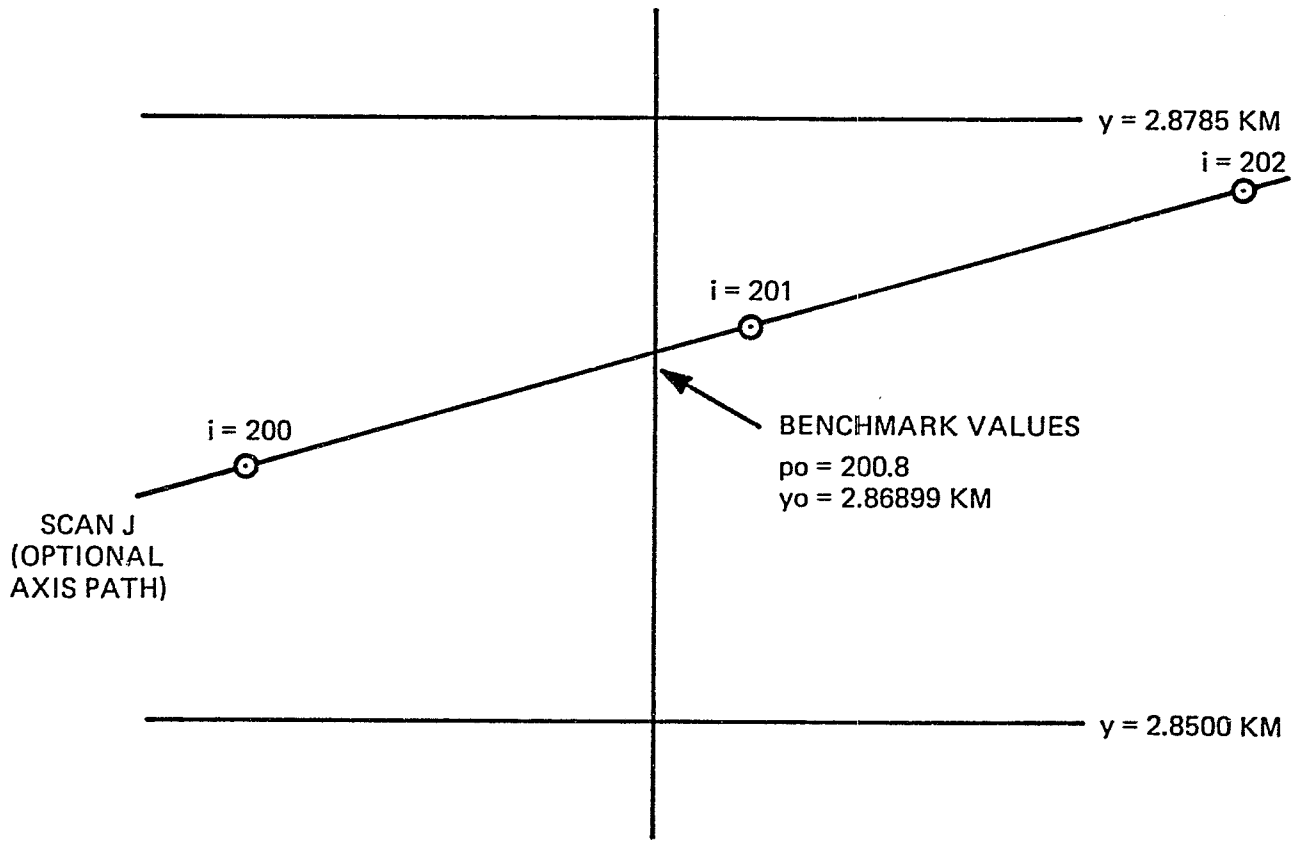

X, Y: OUTPUT COORDINATE SYSTEM
i : SAMPLE NUMBER OF ODD DETECTORS
RELATIVE TO SCAN START

There are 374 scans identified with each WRS scene. The first scan is always a forward scan. The benchmarks are calculated at 4 pair of forward and reverse scans: 1 and 2, 125 and 126, 249 and 250, 373 and 374. For each scan, P_0, Y_0 and P_1, Y_1 values are determined for X coordinates: -102.144 km, -72.96 km, -43.776 km, -14.592 km, 14.592 km, 43.776 km, 72.96 km, and 102.144 km.

Benchmark values can be determined for other scans of X-coordinates by interpolating the benchmark matrix data. Actual scan times must be used during this interpolation process.

The benchmark matricies are generated using WRS scene center parameters, map projections, TM alignment, smoothed ephemeris data, and scan start times for the evaluated scans. The processing assumes that the attitude control maintains perfect pointing of its controlled axis and that the scan mirrors have linear angular motion with nominal active scan time. These assumptions are removed when high frequency matricies are combined with the benchmark matricies.

High Frequency Matricies combine the ADP altitude deviation data and the Mirror Scan deviation data. There are two high frequency matricies: along scan and cross scan. The along-scan High Frequency Matrix has 35 data values with 0.002 second spacing for each of the 374 scans comprising a WRS scene. These high frequency values are created by summing the scan mirror deviations and the ADP roll data. Figure 3-9 illustrates which high frequency values are used for a given scan. For each scan, 35 high frequency values (0.070 seconds) are supplied starting with two values preceeding the scan start time. This allows the high frequency data to be interpolated to the scan start time. With two high frequency samples also needed for end scan time interpolation, the 35 values guarantees 0.066 seconds of usable data during an active scan.

FIGURE 3-9
ALONG SCAN HIGH-FREQUENCY MATRICES

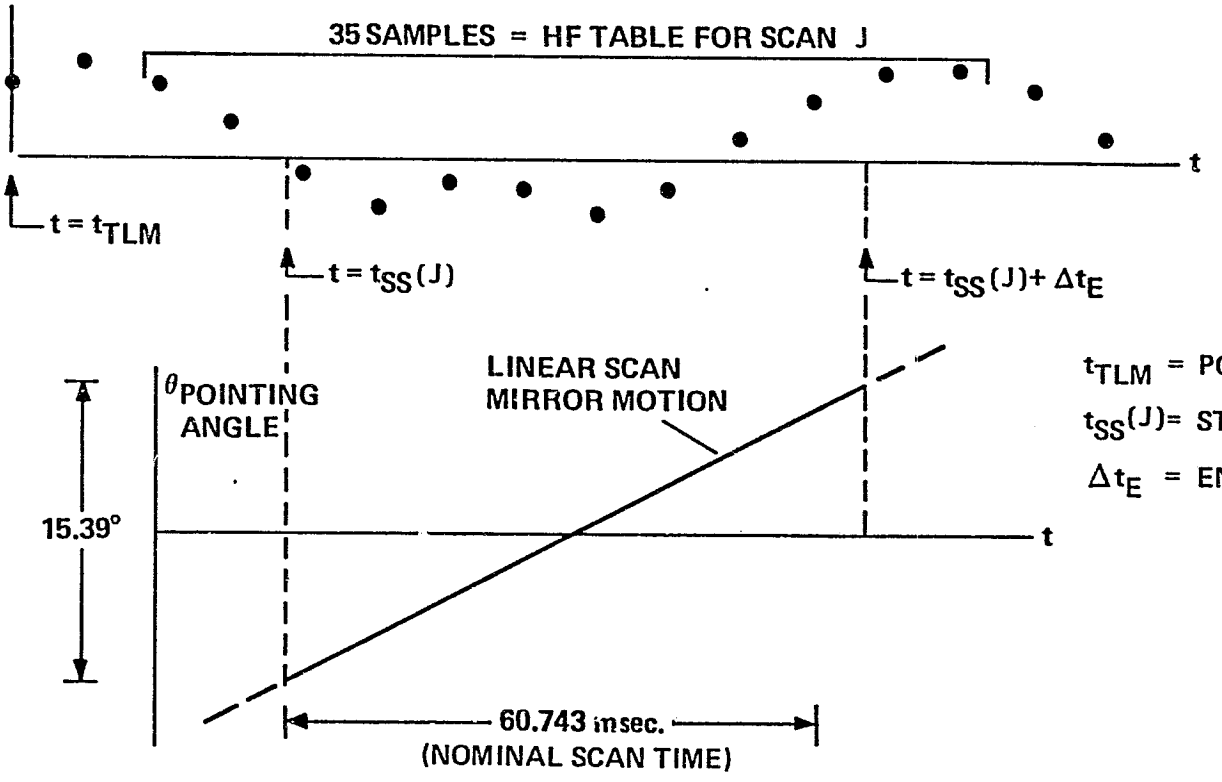

t_{TLM} = PCD TELEMETRY START TIME

$t_{SS}(J)$ = START SCAN TIME, SCAN J

Δt_E = END SCAN TIME INTERVAL

ALONG-SCAN $\theta_{HF} = \theta_\epsilon + \theta_{ROLL}$; θ_ϵ = SCAN MIRROR NONLINEARITY

HF: HIGH FREQUENCY

The Cross Scan High Frequency Matrix by combining cross scan mirror deviations (σ_E), pitch (θ_{pitch}) and yaw (θ_{yaw}) attitude deviations:

$$\Theta_{HF} = \sigma_E - \theta_{pitch} \cdot \cos\theta - \theta_{yaw} \cdot \mathrm{SIN}\theta$$

where θ is the scan mirror point angle relative to mid-scan. The matrix has 35 entries, evaluated every 0.002 sec, for each of the 374 scans comprising the WRS scene. The selection of the 35 points is performed analogously to the Along Scan High Frequency Matrix.

Detector focal plane location parameters define the along scan and cross scan off-axis location of the detector elements. These parameters include the effective geometric error due to TM timing delays. These data items are fixed in a static data base and include the nominal point vector scan rate across the output projection, nominal along scan focal plane band locations, along scan focal plane detector locations, nominal cross scan focal plane band location and the cross scan focal plane detector spacing.

The Data Formatter-Processor (DFP) performs the function of nominally aligning odd-even detectors and spectral bands arrays within a scan. This operation is performed on an integer detector sample basis while the TM archive imagery is being formatted. The DFP odd detector shifts indicate the magnitude of this shift for each scan direction.

An example of SCD usage is given in Appendix A.

3.2 Control Point Processing

Control point processing estimates the low frequency errors due to undertainties in the input data that was used to generate the SCD. Measurements for estimating the SCD errors are provided by control point mislocations in the imagery generated by resampling TM data using the SCD.

The SCD geometric errors fall into two broad categories: (1) High frequency errors and (2) Bias and drift errors. High frequency errors cannot be removed using control points. These errors are principally caused by:

- High frequency (greater than 0.01 Hz) attitude deviation measurement and processing errors
- TM scan repeatability errors
- Computational and linearization errors made in generating and using SCD

The effect of bias and drift errors can be substantially reduced through control point processing. These errors are caused by data uncertainties in:

- Ephemeris
- Absolute time
- Low frequency attitude
- TM alignment

The basic approach used in estimating these errors is to model their variation over time and then use control point mislocation measurements to estimate state variable parameters of these models. In this manner, significant reduction to the number of control points needed can be achieved,especially when a group of consecutively imaged scenes are processed. This approach also provides reduced sensitivity to control point location distribution.

Information from regions with large numbers of control points can be propagated to image regions with few control points.

Drift and Bias Errors in SCD

The spacecraft ephemeris data has been smoothed with a J2 orbit model during Payload Correctin Processing. This process does not significantly increase the ephemeris uncertainty described in Section 2.1. It does provide a smoothed analytic ephemeris with known error dynamics with respect to true ephemeris. Thus, dynamic equations can be written defining ephemeris error propagation in time.

The relative timing between scan data and attitude deviation data is tightly controlled by the spacecraft oscillator. However, absolute time errors effectively create additional uncertainty in ephemeris, especially in the rapidly changing along track component. Absolute time errors present no additional processing complexity over those of the ephemeris uncertainty.

The spacecraft attitude control system has an inertial attitude uncertainty (0.01 degrees (1σ)) due to star tracker uncertainty, star tracker misalignment, non-linear gyro drift and ephemeris uncertainty. The gyros measure any attitude deviations below 2 Hz and attitude control stability is not a significant factor. The dynamics of the pointing uncertainty are well understood and can be accurately modeled as shown in Figure 2-5.

The alignment between the TM and the Attitude Control Systems reference axis is uncertain due to alignment measurement error, differing structural temperatures at time of alignment measurement and during orbital conditions, reassembly of the

Multimission Spacecraft and Instrument Module at the launch site, and structural stresses during launch. In addition to this unknown alignment bias, structural temperature variation from cyclic operation of spacecraft subsystems will cause the alignment to vary over time. A good characterization of dynamic alignment is difficult to obtain. The system level design approach has been to estimate alignment effects during control point processing. The processing has been parametrically exercised with flexible correlated noise models such as that shown in Figure 2-6.

Landsat-D Control Point Concept

The Landsat-D concept underlying the use of control points is shown in Figure 3-10. The Landsat spacecraft is maintained in an orbit which generates a repeatable ground track. An orbital ground track is repeated every 16 days. Each time a World Reference System scene is imaged, the output product should be temporally registered to previous output products.

If Systematic Correction Data were used to generate output products, the resulting imagery would be internally consistent (with the exception of high frequency and drift errors), but would exhibit large offsets when compared temporally. Control points are used to establish temporal registration by estimating the spacecraft errors (ephemeris, time, low frequency attitude and alignment errors) needed to force each overflight to register with the reference interval imagery.

In order to establish a Geodetic basis for output products, the reference interval is first rectified to a geodetic reference. Landsat-D uses available maps (called Standard Maps) as the geodetic reference. This rectification is accomplished during a Control Point Library Build process. The reference interval imagery is corrected using SCD's. Then mislocations between the corrected reference interval and geodetic control point locations from the Standard Maps are used to estimate the spacecraft errors. All Landsat-D TM processing is performed using a standard geoid. Thus, Geodetic Control point information from the Standard Maps are converted to latitude, longitude and elevation relative to the standard geoid. The elevation is needed so that spacecraft errors can be properly estimated. The spacecraft error effects are removed from the benchmark matrices of the SCD's creating Geodetic Correction Data (GCD). Although the elevations of Geodetic Control points were used in estimating spacecraft errors, during resampling it is assumed that all TM detector samples fall on the standard geoid and earth topographical effects are not considered.

FIGURE 3-10
CONTROL POINT CONCEPT

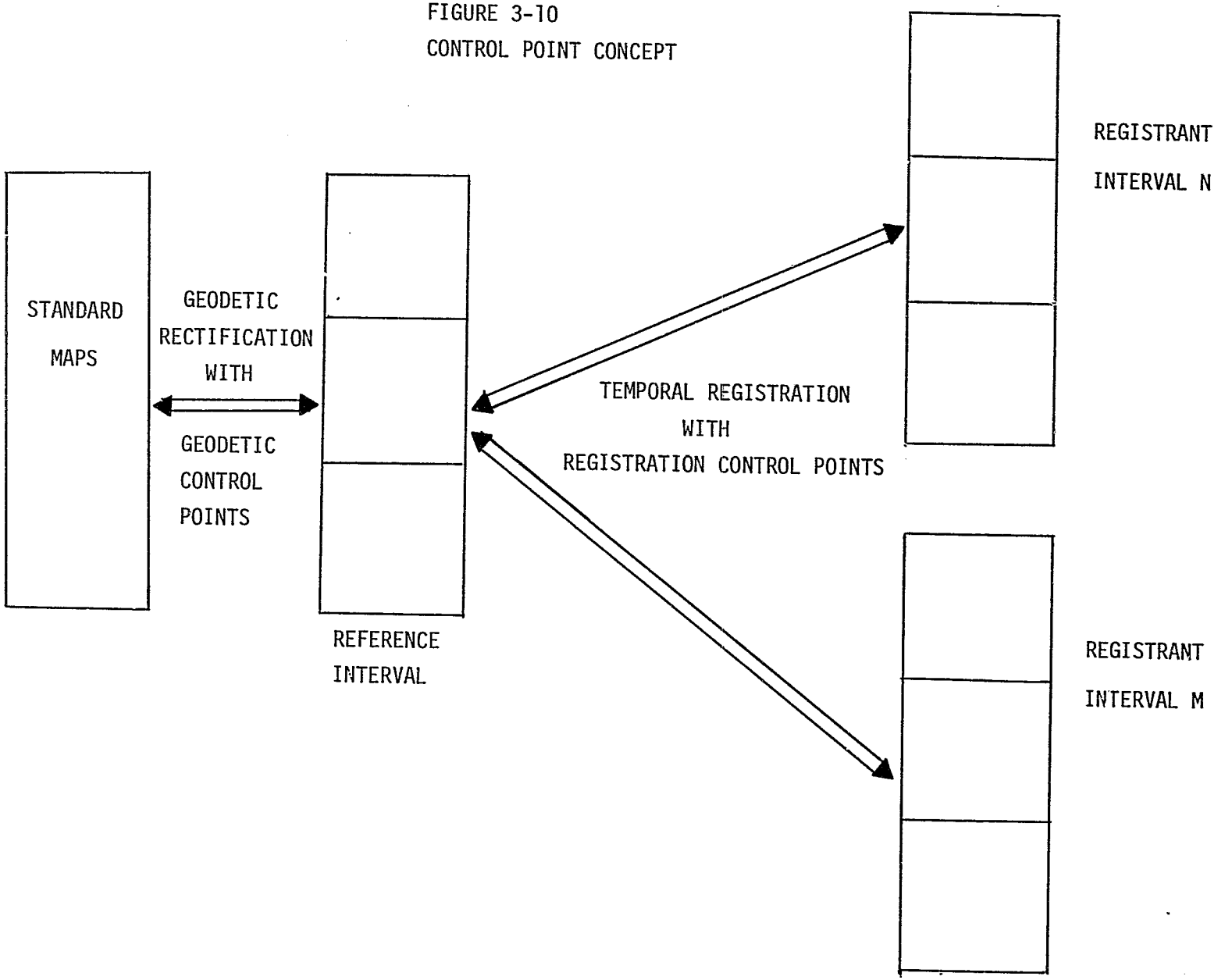

The control point library for the reference interval can now be constructed. It consists of registration control point chips which are 32 pixel by 32 line sections of SCD corrected reference interval imagery. At a defined location on the control point chip, the latitude and longitude and elevation are defined relative to the standard geoid. The elevation information is derived from the standard maps and the latitude and longitude are derived using the GCD's for the reference interval. These registration control points are used to determine the mislocations between the reference interval and all subsequent passes over the reference interval.

Control Point Processing Flow

An overview of the Control Point Processing Flow is shown in Figure 3-11. Payload Correction Processing has generated a set of SCD's for scenes comprising the interval to be processed. The SCD along with the control point latitude, longitude and elevation information from the control point library are used to determine the expected control point location in the unprocessed TM imagery. Control point search neighborhoods are then extracted from the unprocessed imagery. The extracted neighborhood is sufficiently large to generate a 128 pixel by 256 line section of product imagery which is centered on the expected control point location. With this sizing, the 32 pixel X 32 line control point chip can be found in the control point neighborhood even for three sigma ephemeris, time, attitude, and alignment errors. The extracted search neighborhood imagery is first radiometrically corrected using look-up tables (RLUT) and then geometrically corrected using the SCD.

The resultant control point search neighborhood is then digitally correlated with the corresponding control point chip from the control point library. This correlation involves gradient enhancement of edge features in both the control point chip and neighborhood to improve correlation success over time; a rejection ctriteria is applied which provides for correlation peak and surrounding correlation value examination; and a subpixel location routine is applied to accepted control points. To meet specified temporal registration performance, the control point location procedure

FIGURE 3-11

CONTROL POINT PROCESSING FLOW

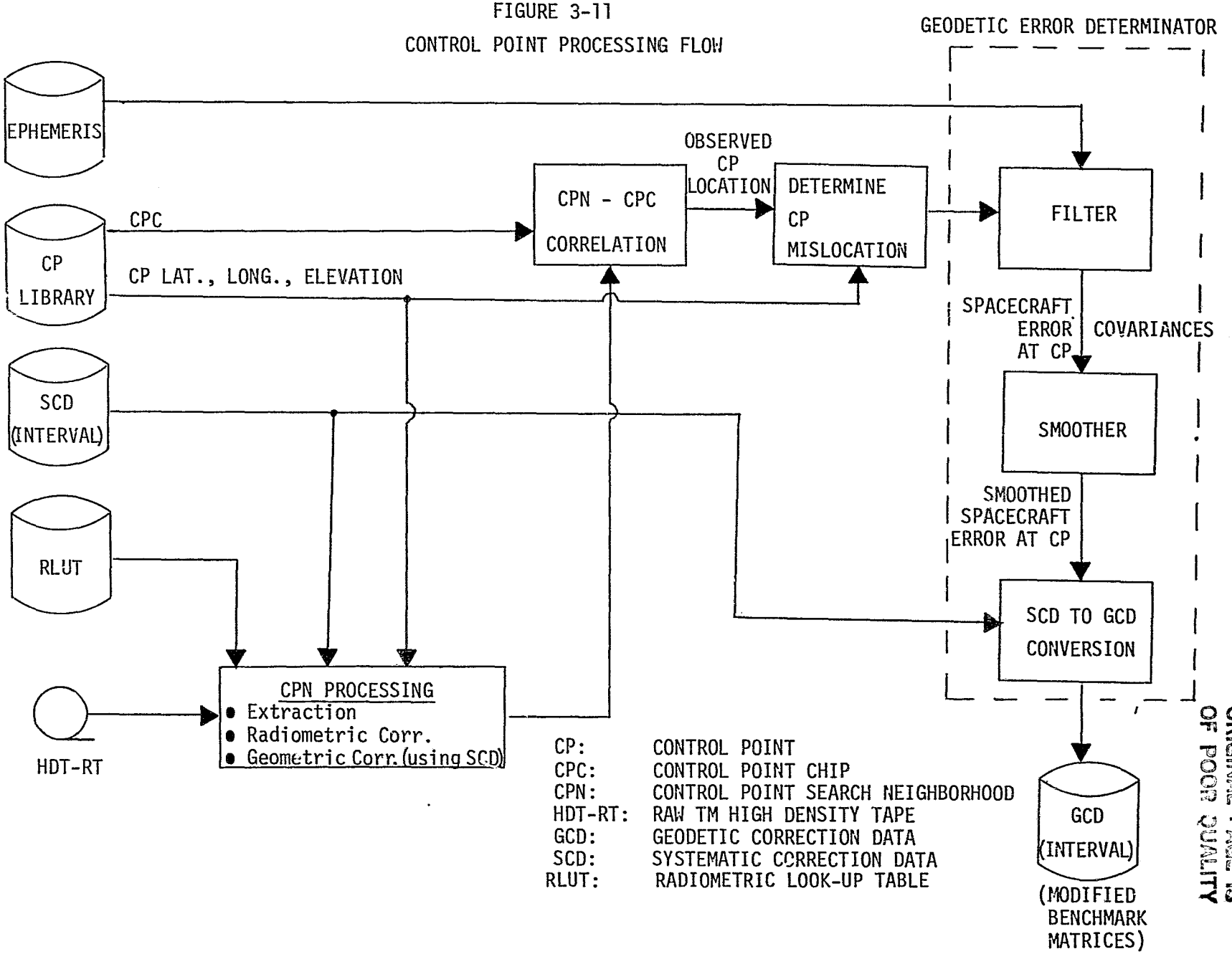

must be capable of finding chip to neighborhood match points with an errors of less than 0.1 pixel (1σ).

Next, the control point mislocation is determined. This is the error on the output projection between the expected control point location (determined from the latitude, longitude and elevation) and the actual observed control point location in the SCD processed control point neighborhood.

The Geodetic Error Determinator (GED) is a set of processing software which uses the control point mislocation information to update the SCD's in the interval. GED processing has three basic steps: Filtering, smoothing, SCD to GCD conversion. During filtering, the mislocation results are used to estimate state variables of a spacecraft error model. The spacecraft error state variables are position error (x,y,z), velocity error $(\dot{x},\dot{y},\dot{z})$, attitude error (R,P,Y) and attitude rate error $(\dot{R},\dot{P},\dot{Y})$. After simulation analysis, it was discovered that alignment and attitude errors could be combined into a single set of 6 attitude variables. The filtering proceeds by propagating the spacecraft error state to a control point time. The spacecraft state is estimated as a weighted average of the state estimated using the mislocation information and the propagated state. The smoother adjusts the spacecraft error state using the control point information over the entire interval. The SCD to GCD conversion processing applies the spacecraft error states to adjust the benchmark matrix values of the SCD's. The adjustments remove the measured error effects from the SCD and the result is called Geodetic Correction Data (GCD).

As previously mentioned, the control point library build uses control point latitude, longitude and elevation information derived from standard maps to correct the SCD's of a reference interval. The mislocations between the map information and the observed location on SCD processed TM imagery is used with the Geodetic Error Determination Software to perform the GCD generation. Then 32 pixel by 32 line control point chip image segments are extracted from the SCD corrected imagery. A location within the chip is assigned a latitude and longitude on the standard geoid using the GCD, and an elevation is assigned using the standard maps. The chip and location information are stored into a control point library which is used to process all subsequent passes over the reference interval.

3.3 Geometric Correction Processing

Geodetic Correction Data locates TM detector samples on the output projection system. This information is used during Geometric Correction Processing to resample the detector samples, placing them on the output grid locations as indicated in Figure 3-12.

An output scene may be generated using either of two resampling methods: Nearest Neighbor and Cubic Convolution. Both resampling types are implemented in a two step process which is illustrated for cubic convolution in Figure 3-13. This Figure shows the resampling process without consideration of scan gap problems. First, samples of a given detector (input pixels) are resampled to output projection column locations. This resampling occurs in one dimension along a line of detector samples (called a scan line). Such resampled values are called hybrid pixels and the process that generates the hybrid pixels is called x-resampling. Next, single dimension resampling is performed along each output projection column using the hybrid pixels. This is called y-resampling and the result is a resampled value called an output pixel. Cubic convolution uses four pixels in the resampling process. The applied weights are those of a cubic spline and are shown in Figure 3-14. Nearest Neighbor interpolation chooses the closest pixel value for each resampling step.

FIGURE 3-12

TM GEOMETRIC CORRECTION PROCESS OVERVIEW

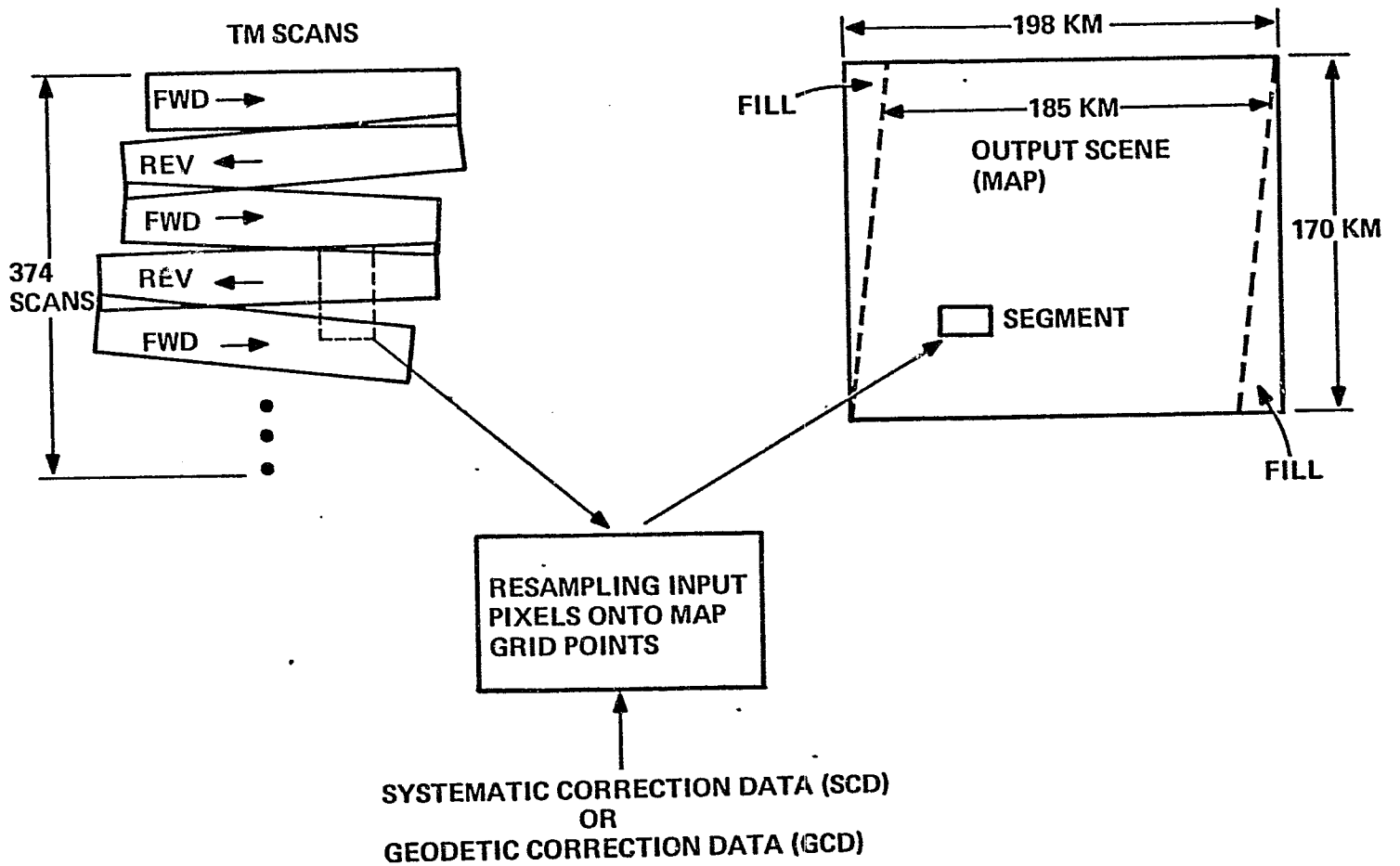

FIGURE 3-13

TWO-DIMENSIONAL CUBIC CONVOLUTION RESAMPLING

- X-RESAMPLING: GENERATE HYBRID PIXELS
- Y-RESAMPLING: GENERATE OUTPUT PIXELS

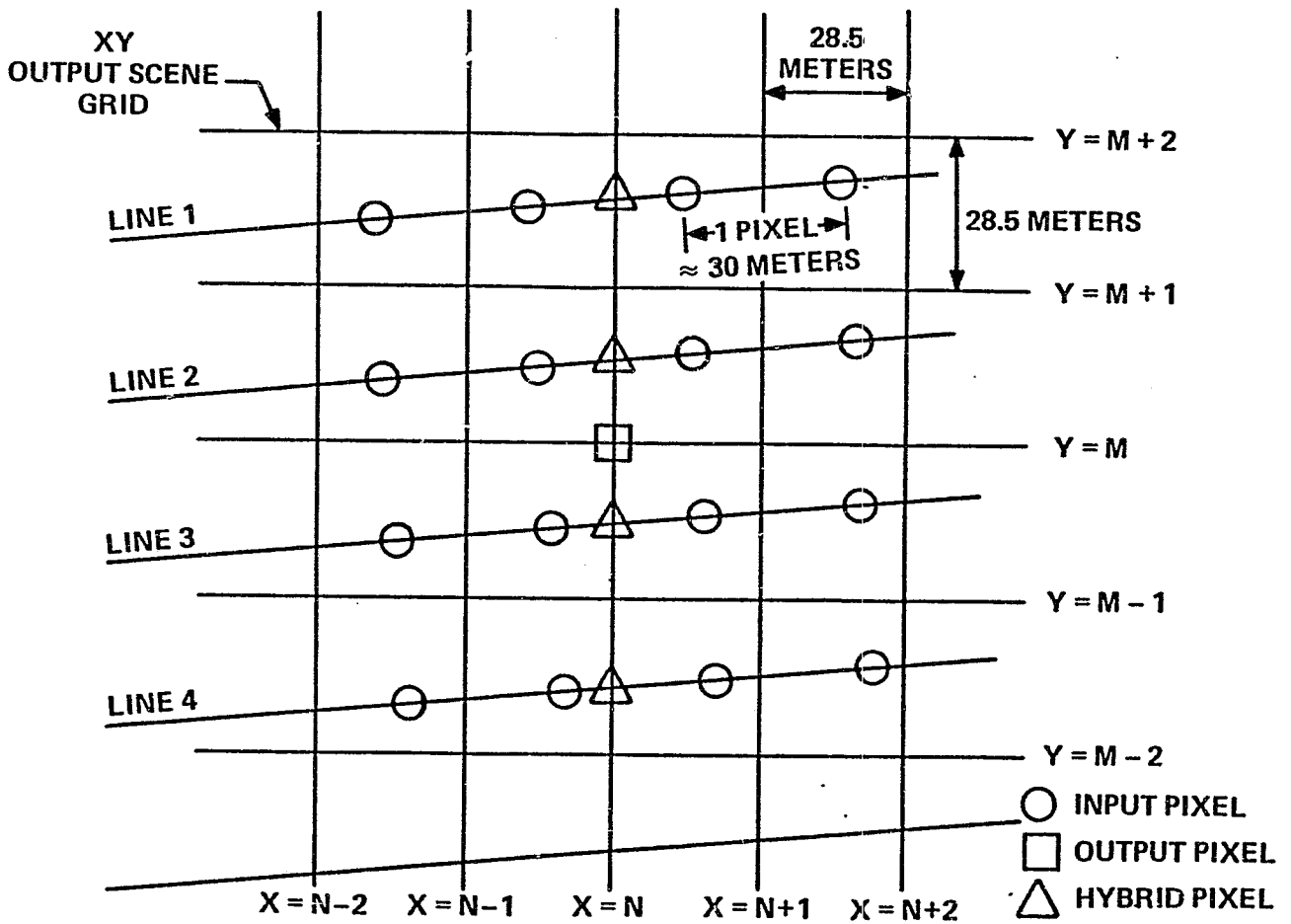

FIGURE 3-14

ONE-DIMENSIONAL CUBIC CONVOLUTION RESAMPLING

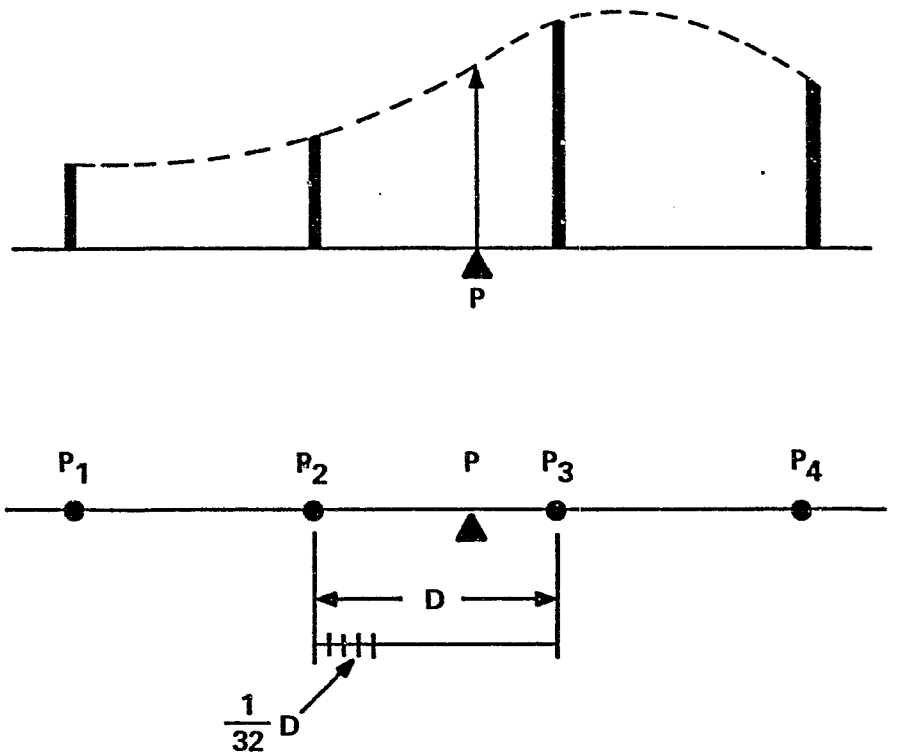

- $P = P_1W_1 + P_2W_2 + P_3W_3 + P_4W_4$
- 32 SETS OF WEIGHTING COEFFICIENTS (W_1, W_2, W_3, W_4) FOR 32 SUB-INTERVALS
- OUTPUT PIXEL LOCATION PRECISION TO (1/64) PIXEL IN RESAMPLING COMPUTATION
- INPUT PIXELS MUST BE EQUALLY SPACED

The TM scan gap error, described in Section 2.3, causes additional complexity for the resampling processing. With MSS processing, acceptable geometric error results from assuming that the sample spacing along a scan line and the spacing between scan lines is equal over a limited region of imagery. With TM processing the gap spacing must be considered. The system throughput requirements place severe limitations on the resampling processing implementation. There are nearly 3×10^8 output pixels in a TM scene. The ground processing requirements translate to an average processing rate of 750,000 pixels/second for resampling. Generation of every pixel requires at least 8 integers multiplies and 6 adds when using cubic convolution. To meet these high processing rates, a dedicated processor is used to implement the arithmetic pipeline resampling procedure. The processor is called a Geometric Correction Operator (GCO). Figure 3-15 defines the scan parameters of gap size, gap skew and scan line skew. These parameters specify the geometry between scans an between a scan and the output grid. The GCO generates output segments of 128 pixels (detector samples) by approximately 17 lines and Table 3-1 shows the GCO capability and worst case conditions for the scan parameters.

When cubic convolution resampling is used, the GCO implements a three-pass process to resample the gap region between two scans. The first pass is called x-resampling. It generates hybrid pixels aligned along output grid columns by using cubic convolution resampling along input lines as previously described.

FIGURE 3-15

SCAN GAP, GAP SKEW AND SCAN LINE SKEW

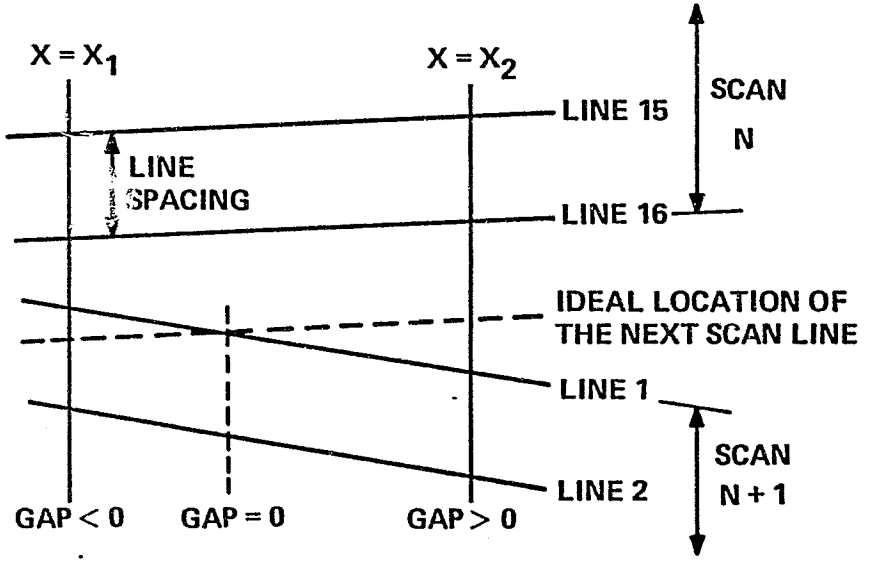

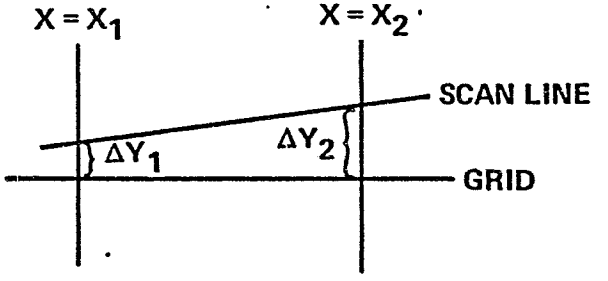

- SCAN GAP IS CAUSED PRIMARILY BY ALTITUDE VARIATION, SCAN LINE CORRECTOR SCAN RATE, SPACECRAFT PITCH AND YAW JITTER.
- GAP SIZE = (SPACING BETWEEN LINE 16 AND LINE 1) — LINE SPACING
- GAP SKEW = $\frac{\text{GAP SIZE } (X_2) - \text{GAP SIZE } (X_1)}{X_2 - X_1}$
- SCAN LINE SKEW = $\frac{\Delta Y_2 - \Delta Y_1}{X_2 - X_1}$
- X_1, X_2 = LEFT, RIGHT SIDE OF OUTPUT SEGMENT
- $X_2 = X_1 + 128$

TABLE 3-1

GEOMETRIC CORRECTION OPERATOR (GCO) GAP HANDLING CAPABILITY

	WORST CASE (IN PIXELS)	GCO CAPABILITY (IN PIXELS)
GAP SIZE	–2.8 TO 2.0	-5 TO 3
GAP SKEW OVER 128 OUTPUT PIXELS	–0.42 TO 0.42	-2 TO 2
TM SCAN LINE SKEW OVER 128 OUTPUT PIXELS	–1.0 TO 1.0	-2 TO 2

Figure 3-16 shows the hybrid pixel locations for two scans after x-resampling. The generation of samples at grid locations requires the use of four unevenly spaced hybrid pixels between lines 15 and 18. The resampling weights to be applied in this gap region are a function of two parameters: the distance between the grid point and scan line 16 and the gap size. Note that the line spacing within scan N and scan N+1 may be assumed equal.

When performing high speed resampling, it is necessary to use precomputed sets of four weights. This avoids the significant overhead of generating the weights during processing. The weight sets are calculated every 1/32 pixel. In order to reduce the number of weight sets and to simplify the processing, an intermediate resampling pass called sweep extension (or E-resampling) is used. Starting with the hybrid pixels from scans N and N+1, scan N is extended (lines 17E, 18E, etc.) using a spline interpolation along output columns as shown in Figure 3-16. This extension continues until output grid pixels can be generated using cubic convolution with the hybrid pixels of scan N+1 alone. The extension pass requires weight sets which are a function of one parameter, the gap size, because the extension lines are spaced an integer number of line spacings below line 16.

The last resampling pass (y-resampling) is then performed after sweep extension. The output grid pixels can be generated using cubic convolution along the output grid columns as with the zero gap case. The hybrid pixels from scan N and the extension pixels are used in this pass.

The gap region between scans N+1 and N+2 are similarly processed by extending scan N+1 and performing y-resampling starting from the point at which processing of scan N was terminated.

FIGURE 3-16

GENERATE SCAN EXTENSION LINE PIXELS

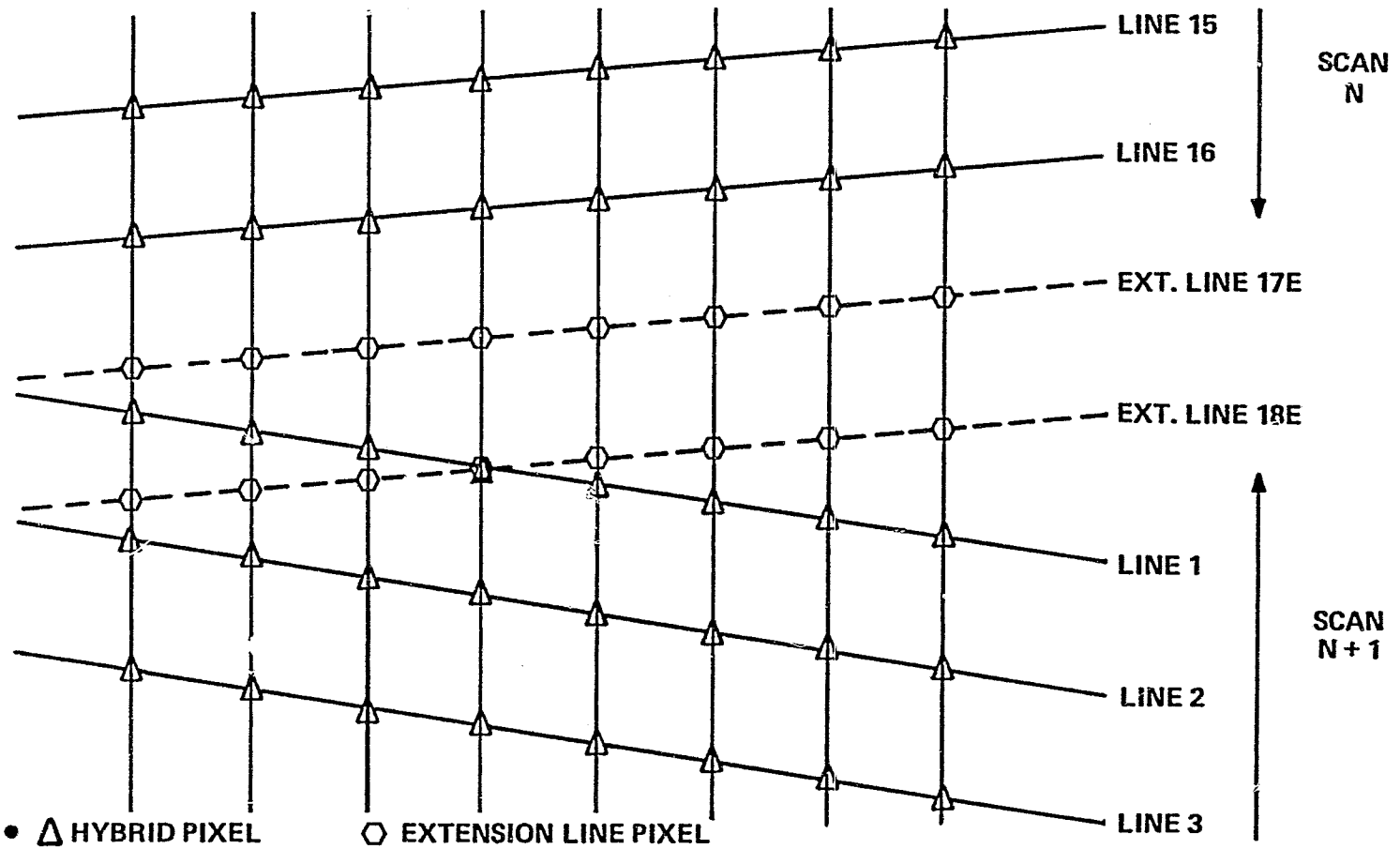

- △ HYBRID PIXEL ⬡ EXTENSION LINE PIXEL
- EXTENSION PIXELS ARE GENERATED WITH TWO HYBRID PIXELS ABOVE AND TWO HYBRID PIXELS BELOW
- PIXEL LOCATION PRECISION TO (1/64) PIXEL IN RESAMPLING COMPUTATION

By appropriately defined weight sets, both positive and negative gaps can be accommodated using sweep extension. This approach degenerates into standard cubic convolution when the gap size is zero. The sweep extension resampling weights are also cubic spline interpolations with weights defined as shown in Figure 3-17.

FIGURE 3-17

SPLINE INTERPOLATION FORMULA

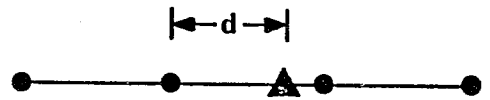

● INPUT PIXEL LOCATION

▲ DESIRED PIXEL LOCATION

	CUBIC CONVOLUTION WEIGHT FORMULAS	CUBIC SPLINE WEIGHT FORMULAS
W_1	$-d(1-d)^2$	$\frac{2a_1}{ch_1h_2} f_1f_2f_3 - \frac{1}{ch_1} g_1g_2g_3$
W_2	$(1-d)(1+d-d^2)$	$-\frac{1}{ch_1} f_1f_2f_3\left(1+\frac{2a_1}{h_2}+\frac{2a_1}{h_1}\right)+\frac{f_3}{h_2}+\frac{1}{c}g_1g_2g_3\left(\frac{2a_0}{h^2_2}+\frac{1}{h_1}+\frac{1}{h_2}\right)$
W_3	$d(1+d-d^2)$	$\frac{1}{c}f_1f_2f_3\left(\frac{2a_1}{h^2_2}+\frac{1}{h_2}+\frac{1}{h_3}\right)-\frac{1}{ch_2}\left(g_1g_2g_3\right)\left(1+\frac{2a_0}{h_2}+\frac{2a_0}{h_3}\right)+\frac{g_3}{h_2}$
W_4	$-d^2(1-d)$	$-\frac{1}{ch_3} f_1f_2f_3+\frac{2a_0}{ch_2h_3} g_1g_2g_3$

$f_1 = X_3 - X - h_2$ $\quad g_1 = X - X_2 - h_2$ $\quad h_1 = X_2 - X_1$ $\quad a_0 = h_1 + h_2$

$f_2 = X_3 - X + h_2$ $\quad g_2 = X - X_2 + h_2$ $\quad h_2 = X_3 - X_2$ $\quad a_1 = h_2 + h_3$

$f_3 = X_3 - X$ $\quad g_3 = X - X_2$ $\quad h_3 = X_4 - X_3$ $\quad c = 4a_0a_1 - h^2_2$

APPENDIX A
SEGMENT DATA CALCULATION USING SCD

This Appendix describes how Systematic Correction Data is combined to generate a set of benchmark type data called segment data. Segment data combines all information in the SCD to determine the location of each TM detector sample on a dense grid system.

Output Data (single map projection, single scene)

The output data of the segment calculation consists of sample times (input pixel numbers) $p_{m,n}(i,j)$ and output projection y-coordinates $y_{m,n}(i,j)$ for detector numbers:

$n = 1, 2, \ldots, 16$ (or 4 for Band 6)

at the GCO segment edge defined by:

$i = 1, 2, \ldots, 57$ = x-coordinate index

$j = 1, 2, \ldots, 374$ = scan number

$m = 1, 2, \ldots, 7$ = band number.

The x-coordinate index corresponds to:

$X = 128\ (28.5)[-28 + (i-1)]$ meters.

It has been assumed that the individual detectors in each band's detector array are uniformly spaced on the focal plane in the cross-scan (along-track) direction. This allows reducing the display y-coordinate data for Band m to two values: $y_{m,1}(i,j)$, the y-coordinate for Detector 1, and $\Delta y_m(i,j)$, the y-coordinate spacing between adjacent detectors.

Note that the number of scans in the SCD (374) is 16 scans more than will nominally fill the 170 km high output scene. The SCD "scene" is larger to enable geometric correction of 256 X 256 pixel neighborhoods of geodetic control points near the top

and/or bottom edges of the output scene. Also, since the total along-track error is expected to be no greater than ± 3 km, the same SCD can be updated to geodetic correction data (GCD) following geodetic correction processing by simply adjusting the benchmark matrices.

Procedure

1. Interpolate sparse matrices - For each combination of i and j, interpolate between the appropriate benchmark matrix rows to compute the intermediate benchmarks

   for: $p_0(i,j)$, $y_0(i,j)$, $p_1(i,j)$, $y_1(i,j)$.

   $i = 1, 2, \ldots, 57$ = x-coordinate index

   $j = 1, 2, \ldots, 374$ = scan number

   In the three benchmark matrix rows having the same scan direction and surrounding the j^{th} scan, first interpolate horizontally to x-coordinate index i using 4-point cubic convolution. Then interpolate p_0, y_0, p_1, y_1 vertically to scan start time $\tau(j)$ using 3-point quadratic interpolation to determine the intermediate benchmarks at (i,j).

2. Sample time (pixel) adjustments (for each m,n)

A. Nominal band along-scan

$$\Delta t_1 = -\Delta\theta(m)/\dot{\theta}_{eff}$$

B. HF along-scan

$$\Delta t_2 = -\hat{\theta}_{HF}(t_2)/\dot{\theta}_{eff}$$

where:

$t_2 = t_o + \Delta t_1 + \Delta t_2$ ($t_2 = t_o + \Delta t_1$ initially, then iterated)

$t_o = p_o(i,j)T_p$

T_p = pixel sample period = 9.611 μsec

$\hat{\theta}_{HF}(t_2)$ = value [rad] interpolated from HF along-scan array corresponding to time t_2

C. HF cross-scan

$$\Delta t_3 = -U(i,j)\ \hat{\sigma}_{HF}(t_2)/\dot{\theta}_{eff}(k)$$

where:

$U(i,j) = -[p_1(i,j) - p_o(i,j)]/\sigma_1$

σ_1 = cross-scan angle used to compute p_1 [rad]

$\hat{\sigma}_{HF}(t_2)$ = value [rad] interpolated from HF cross-scan array corresponding to time t_2 (from step B)

D. Detector along-scan

$$\Delta t_4 = -\delta\theta(m,n,k)/\dot{\theta}_{eff}(k)$$

E. Detector cross-scan

$$\Delta t_5 = -U(i,j)\delta\sigma(m,n)$$

where

$\delta\sigma(m,n) = \delta\sigma(m) + [n - (NDET) + 1)/2] \cdot d\sigma(m)$

NDET = 16 (= 4 for Band 6)

Finally, the detector sample time (input pixel) for Detector n, Band m is:

$$p_{m,n}(i,j) = p_o(i,j) + \sum_{i=1}^{5} \Delta t_i/T_p$$

3. <u>Y-coordinate adjustments</u> (for each m,n)

A. High-frequency cross-scan

$$\Delta y_1 = S(i,j)\ \hat{\sigma}_{HF}(t_2)$$

where

$S(i,j) = [y_1(i,j) - y_o(i,j)]/\sigma_1$

B. Detector cross-scan

$$\Delta y_2 = S(i,j)\delta\sigma(m,n)$$

The display y-coordinate for Detector n, Band m is then:

$$y_{m,n}(i,j) = y_o(i,j) + \Delta y_1 + \Delta y_2$$

More specifically, the Detector 1 y-coordinate $y_{m,1}(i,j)$ and the y-coordiante spacing are required:

$$\Delta y_m(i,j) = y_{m,n+1}(i,j) - y_{m,n}(i,j) = S(i,j) \cdot d\sigma(m)$$